AIMS Mathematics, 11(3): 6834–6865.
DOI: 10.3934/math.2026282
Received: 29 January 2026
Revised: 01 March 2026
Accepted: 09 March 2026
Published: 17 March 2026

http://www.aimspress.com/journal/Math

Research article

A new block censoring scheme: comparative assessment of likelihood and spacings methods for Weibull distribution with an application to cancer data

Mazen Nassar[1,2,*] **and Refah Alotaibi**[3]

[1] Department of Statistics, Faculty of Science, King Abdulaziz University, Jeddah 21589, Saudi Arabia

[2] Department of Statistics, Faculty of Commerce, Zagazig University, Zagazig, Egypt

[3] Department of Mathematical Sciences, College of Science, Princess Nourah bint Abdulrahman University, P.O. Box 84428, Riyadh 11671, Saudi Arabia

* **Correspondence:** Email: mmohamad3@kau.edu.sa, mezo10011@gmail.com.

Abstract: In reliability experiments conducted across multiple groups, prolonged test durations and heterogeneity among groups can substantially reduce efficiency and affect statistical inference. This study has proposed a new censoring design that combines block experimentation with an improved adaptive progressive Type-II hybrid termination rule to ensure controlled test duration while maintaining sufficient failure information. The proposed framework generalizes several existing censoring schemes and allows independent groups to operate under flexible stopping conditions. Assuming Weibull lifetimes with a common shape parameter and group-specific scale parameters, parameter estimation and reliability characteristics were obtained using maximum likelihood and maximum product of spacings methods. Both point and interval estimators were developed. To quantify heterogeneity across groups, a new measure based on confidence interval overlap, called the coverage similarity index, was introduced. Simulation results showed that the maximum product of spacings method generally provides more accurate estimation for scale-related quantities and reliability measures, while maximum likelihood performs slightly better for the shape parameter and mean time to failure. The proposed methodology was illustrated using cancer survival data from ovary, breast, and kidney groups, where meaningful heterogeneity was detected. The findings confirm the practical value of the proposed design and highlight the importance of accounting for group-level variation in reliability and survival analysis.

Keywords: block improved adaptive progressive Type-II hybrid censoring scheme; Weibull distribution; reliability characteristics; spacings function; coverage similarity index

Mathematics Subject Classification: 62F10, 62F15, 62N01, 62N05

1. Introduction

In reliability and survival analysis, censored data arise naturally when complete information on all experimental units cannot be obtained within the available time or under the given experimental conditions. In many life-testing experiments, especially when dealing with highly reliable or long-lived products, observing all failure times may be prohibitively time-consuming, economically infeasible, or even physically impractical. To overcome these challenges, censoring schemes are adopted to allow early termination of experiments while still retaining sufficient information for statistical inference. Consequently, censoring has become a fundamental component of modern reliability experimentation and lifetime modeling, enabling efficient inference about underlying lifetime distributions even when the sample is incomplete. Throughout this study, the terms "reliability" and "survival" are used interchangeably. In reliability analysis, the reliability function (RF) represents the probability that a unit survives beyond a specified time, whereas in biomedical contexts, the survival function conveys the same probabilistic meaning. Since both concepts are mathematically equivalent under lifetime modeling, we adopt the two terms interchangeably depending on the application context.

1.1. Progressive and adaptive progressive hybrid censoring

In practice, various censoring plans have been proposed to address different experimental settings, each characterized by its own stopping rules and operational advantages. Among these, progressive censoring has attracted substantial attention due to its flexibility and efficiency in utilizing available information. In a progressive Type-II censoring (PTIIC) scheme, the experiment begins with n identical units placed on a life test, and the test continues until a predetermined number of failures, say, m ($m < n$), have been observed. At the time of each observed failure, a specified number of surviving units are randomly withdrawn (or censored) from the experiment according to a prearranged scheme $R_1, R_2, \ldots, R_m$, where R_i denotes the number of units removed at the i-th failure time and $\sum_{i=1}^{m} R_i + m = n$. The test is terminated after the m-th failure, and statistical inference is then based on the observed m failure times. The PTIIC scheme has been extensively applied in reliability and lifetime studies due to its adaptability and analytical tractability, see, for example, Ng et al. [1], Kundu [2], and Lee et al. [3]. However, one of the practical limitations of the PTIIC scheme lies in the potentially long duration required to complete the test, particularly when dealing with highly reliable products that fail infrequently. To address this issue, Kundu and Joarder [4] proposed a progressive Type-I hybrid censoring scheme (PTIHCS), which combines the advantages of both PTIIC and hybrid censoring strategies. In this design, the experiment terminates at the minimum of two quantities, $\min(X_m, T)$, where X_m denotes the time of the m-th observed failure and T represents a pre-specified termination time.

The PTIHC scheme presents certain limitations, most notably that the effective sample size, representing the actual number of observed failures, sometimes becomes too small, resulting in a loss of information and a decline in the efficiency of parameter estimation. To overcome this drawback, Ng et al. [5] introduced an adaptive progressive Type-II hybrid censoring (APTIIHC) scheme, in which the

experimental time may extend beyond the predetermined duration T while maintaining a fixed effective sample size m. In the APTIIHC scheme, n identical units are placed on a life test, and the number of failures to be observed is predetermined as m ($m \leq n$). A progressive censoring scheme $(R_1, R_2, \ldots, R_m)$ is preassigned. During the APTIIHC procedure, if the m-th failure occurs before the pre-specified time T (i.e., $X_m < T$), the test terminates at X_m, which coincides with the conventional PTIIC plan. However, if $X_d < T < X_{d+1}$ for some $d = 1, 2, \ldots, m-1$, then the censoring plan is adaptively modified by setting $R_{d+1} = R_{d+2} = \cdots = R_{m-1} = 0$. Consequently, the original censoring scheme $(R_1, R_2, \ldots, R_m)$ is transformed into an adjusted scheme $(R_1, R_2, \ldots, R_d, 0, \ldots, 0, R_m^*)$, with $R_m^* = n - m - \sum_{j=1}^{d} R_j$. This adaptive modification ensures that the experiment always terminates once the predetermined number of failures m has been observed, thereby maintaining the integrity of the design while enhancing its flexibility and efficiency. Recently, the APTIIHC scheme has attracted considerable attention among researchers due to its ability to balance experimental efficiency and inferential accuracy. For comprehensive discussions, methodological developments, and diverse applications, readers may refer to several recent contributions in the literature, including Ren and Gui [6], Haj Ahmad et al. [7], Alotaibi et al. [8], Dutta et al. [9], and Lv et al. [10], among others. A comprehensive overview of adaptive progressive censoring in reliability and survival analysis is provided in the recent review by Nassar [11].

1.2. Improved adaptive progressive hybrid censoring

One of the main limitations of the APTIIHC scheme is its potentially extended testing duration, which can make it unsuitable for products with very high reliability. However, when experimental time is not a pressing concern, the APTIIHC plan continues to serve as a practical and informative framework for statistical inference in lifetime studies. To alleviate the challenge of prolonged test durations, Yan et al. [12] introduced the improved APTIIHC (IAPTIIHC) scheme. This enhanced design guarantees that the experiment concludes within a predetermined time horizon, effectively merging the adaptability of progressive censoring with the logistical advantage of a fixed termination point. Consequently, the IAPTIIHC scheme offers a more balanced approach, improving both the operational efficiency and inferential reliability of life-testing experiments. Consider a life test conducted on n identical units with a predetermined number of observed failures m, two time thresholds $T^{min} < T^{max}$, and a progressive removal design $(R_1, R_2, \ldots, R_m)$. At the i-th observed failure time X_i, $(i = 1, \ldots, m)$, a designated number R_i of surviving units is randomly withdrawn according to the censoring plan. The termination rule of the experiment gives rise to three distinct scenarios. Case I: If $X_m < T^{min}$, the experiment stops at X_m, producing the standard PTIIC sample with m failures. Case II: If $T^{min} < X_m < T^{max}$, the test also ends at X_m; however, after the first d failures occurring before T^{min}, no further removals take place until the m-th failure, at which point all remaining units are withdrawn, yielding the APTIIHC sample. Case III: If $T^{min} < T^{max} < X_m$, the experiment is terminated at T^{max}, and as in Case II, no removals occur after the d-th failure; at time T^{max}, all surviving units are removed simultaneously. In this case, the final bulk removal size equals $n - r - \sum_{i=1}^{d} R_i$, where r denotes the total number of failures observed prior to T^{max}.

In the literature, several authors developed and analyzed estimation issues of many lifetime models using the IAPTIIHC scheme. Dutta and Kayal [13] investigated a competing-risks model with partially observed failure causes under the IAPTIIHC scheme. They derived maximum-likelihood and Bayesian estimators for the model parameters and established asymptotic confidence intervals.

Nassar and Elshahhat [14] examined the Weibull distribution under the same censoring structure, developed both maximum-likelihood and maximum-product-of-spacings estimation methods, and identified optimal censoring schemes to enhance inferential efficiency. Zhang and Yan [15] focused on parameter estimation for the Chen distribution using the IAPTIIHC plan, constructed likelihood and Bayesian estimators, and evaluated their performance through extensive simulation and real-world data applications. Irfan et al. [16] conducted a comprehensive analysis of the Kumaraswamy-G family of distributions within the IAPTIIHC framework, derived point and interval estimators, and proposed optimal test plans under different cost and precision criteria. For more information, see the work of Dey and Kayal [17] and Nassar et al. [18].

1.3. Block censoring methodologies

A notable limitation of the previously discussed censoring schemes arises when it is impractical to observe all experimental units simultaneously. This situation often occurs when the necessary testing equipment is limited, difficult to access, or when monitoring all units by a single observer is infeasible. To overcome such practical constraints, block censoring mechanisms have been proposed by Ahmadi et al. [19] as a more flexible and realistic framework for life-testing experiments. In this framework, a total of n experimental units are partitioned into k groups, each consisting of n_i units ($i = 1, 2, \ldots, k$), such that $\sum_{i=1}^{k} n_i = n$. Each of the k groups is then tested separately using k corresponding testing facilities under predetermined censoring conditions. This structure allows simultaneous or sequential testing across multiple facilities, thereby improving the efficiency and feasibility of life-testing experiments. Ahmadi et al. [19] presented several theoretical and practical results related to the block censoring methodology, particularly in the context of testing k groups with k facilities under conventional Type-II censoring when the lifetimes of the test units follow an exponential distribution. Similarly, Zhu [20] investigated the Weibull distribution under the same framework. In the context of multi-stage censoring designs, Kumari et al. [21,22] introduced the block PTIIC (BPTIIC) scheme and addressed several estimation issues for lifetime models characterized by bathtub-shaped and Kumaraswamy distributions. This scheme provided enhanced flexibility in handling complex reliability experiments by combining the advantages of block and progressive censoring structures. Furthermore, Wang et al. [23] examined the inverted exponentiated exponential competing-risks model within the BPTIIC framework, demonstrating the usefulness of the block-based progressive approach in analyzing lifetime data involving multiple failure causes. In addition, see the work of Singh et al. [24] and Lodhi et al. [25]. Recently, Singh et al. [26] introduced a more flexible block-based censoring design known as the block APTIIHC (BAPTIIHC) scheme. This scheme was constructed to terminate life tests according to the APTIIHC mechanism while incorporating the advantages of block structures to enhance experimental feasibility. Based on the proposed framework, the authors investigated the reliability characteristics of the Weibull distribution and developed point and interval estimators using both classical and Bayesian inference approaches.

1.4. Motivation and contributions of the study

Although the BAPTIIHC scheme offers considerable flexibility in reliability experimentation, it still has the drawback of potentially long test durations, which may limit its practicality for highly reliable products. Motivated by this limitation, the present study aims to propose a more versatile block-

based censoring plan suitable for such situations. The new design, referred to as the block IAPTIIHC (BIAPTIIHC) scheme, integrates the structural advantages of block censoring with the adaptive and time-controlled features of the improved adaptive progressive framework, thereby ensuring efficient testing and reliable inference even when dealing with long-lived products. Although the proposed BIAPTIIHC scheme integrates block censoring with the IAPTIIHC structure, its contribution extends beyond a simple combination of existing designs. The proposed framework establishes a unified block-based adaptive scheme with dual time thresholds, enabling each group to operate under controlled and synchronized termination rules. The fundamental advancement lies in incorporating an upper time threshold within the block structure, thereby ensuring guaranteed termination even in the presence of highly reliable or long-lived units. This feature directly addresses the practical limitation of prolonged test durations that may occur under the conventional BAPTIIHC scheme. Consequently, the BIAPTIIHC scheme provides a balanced design that simultaneously accommodates multi-group experimentation, adaptive censoring flexibility, and strict time control. This integrated structure offers clear operational advantages in reliability and survival studies where both experimental efficiency and termination control are critical considerations.

In this study, we first introduce the proposed censoring scheme and describe the corresponding data structure, followed by the derivation of the joint likelihood function for the observed failure times. Subsequently, we investigate the estimation aspects of the Weibull distribution as the underlying lifetime model and examine several of its key reliability measures, including the RF, hazard rate function (HRF), and mean time to failure (MTTF). Parameter estimation is performed using two well-established classical methods, maximum likelihood (ML) and maximum product of spacings (MPS), through which both point and interval estimators are obtained and comparatively evaluated. In practice, even though testing facilities are often assumed to be identical, the failure times obtained from different facilities may exhibit noticeable variability. Such differences can result from variations in operating conditions, testing procedures, environmental factors, or data collection precision. Therefore, it is more realistic to treat these observations as non-identical records, where the differences across different testing facilities (DDTF) may have significant implications for the accuracy and interpretation of reliability analysis. Deriving statistical inferences regarding the DDTF therefore constitutes another important aspect of the present study. In order to compare the performance of the proposed estimators, a Monte Carlo simulation study was conducted, and one real data application is analyzed to illustrate the practical usefulness of the developed methods.

The remainder of this paper is structured as follows. Section 2 presents the description of the proposed model and formulates the likelihood function under the BIAPTIIHC scheme. Section 3 details the derivation of the ML estimators (MLEs) for the unknown parameters, reliability characteristics (RCs), and DDTF. The MPS estimation approach is developed in Section 4. Section 5 reports the findings of a Monte Carlo simulation study, while Section 6 illustrates the applicability of the proposed methodology through one real data analysis. Finally, Section 7 summarizes the key conclusions and potential directions for future research.

2. Model description and testing methodology

In this section, we first present the Weibull lifetime distribution and its RCs, followed by a detailed description of the BIAPTIIHC scheme and its operational structure.

2.1. Weibull distribution

In this study, we assume that the lifetimes of the tested units follow the Weibull distribution. This distribution, originally introduced by Weibull [27], is among the most widely used models in reliability and survival analysis. Its popularity arises from its exceptional flexibility: by varying the shape parameter β, it can represent decreasing ($\beta < 1$), constant ($\beta = 1$), or increasing ($\beta > 1$) hazard rates. This adaptability has made the Weibull model indispensable across numerous disciplines, including engineering, medicine, communications, meteorology, and materials science. Moreover, the Weibull distribution serves as a generalization of both the exponential distribution (for $\beta = 1$) and the Rayleigh distribution (for $\beta = 2$). Owing to these properties, it is particularly well suited for modeling lifetimes in reliability experiments where the failure behavior evolves over time and constant-rate assumptions are insufficient. Let X be a random variable following a Weibull distribution with scale parameter δ and shape parameter β, denoted as $X \sim \text{Weibull}(\delta, \beta)$. The probability density function (PDF) and cumulative distribution function (CDF) of X are, respectively, given by

$$f(x; \delta, \beta) = \delta\beta x^{\beta-1} e^{-\delta x^{\beta}}, \; x > 0, \; \delta\beta > 0, \tag{2.1}$$

and

$$F(x; \delta, \beta) = 1 - e^{-\delta x^{\beta}}. \tag{2.2}$$

In addition, this study investigates several RCs of the Weibull distribution, namely the RF $R(x; \delta, \beta)$, the HRF $H(x; \delta, \beta)$, and the MTTF $\mu(\delta, \beta)$. For the Weibull distribution with the PDF defined in (2.1), the corresponding RCs are, respectively, given as follows:

$$R(x; \delta, \beta) = e^{-\delta x^{\beta}}, \tag{2.3}$$

$$H(x; \delta, \beta) = \delta\beta x^{\beta-1}, \tag{2.4}$$

and

$$\mu(\delta, \beta) = \frac{\Gamma\left(1 + \frac{1}{\beta}\right)}{\delta^{1/\beta}}. \tag{2.5}$$

Numerous studies have examined the estimation problems associated with the Weibull distribution and its related reliability measures. Notable contributions include those by Ng et al. [28], Guure and Ibrahim [29], and Ajmal et al. [30], among others. For more details, see Kazempoor et al. [31] and Fathi [32]. Over the years, several extensions and generalizations of the Weibull distribution have been proposed to better capture diverse failure behaviors and accommodate various data patterns encountered in practice. For a comprehensive overview of these developments, readers may refer to Murthy et al. [33], Lai et al. [34], and Abdelaziz et al. [35].

2.2. The BIAPTIIHC testing design

Suppose that, in a block censoring framework, a total of n life-testing units are divided into k groups (or facilities), where the i-th group consists of n_i units ($i = 1, 2, \ldots, k$) such that $\sum_{i=1}^{k} n_i = n$. Each facility is assumed to be tested independently under the IAPTIIHC testing methodology, as introduced by Yan et al. [12]. Let m_i ($i = 1, 2, \ldots, k$) denote the number of observed failures in the i-th facility, and let the corresponding progressive censoring plan be represented by $\mathcal{R}_i = (R_{i1}, R_{i2}, \ldots, R_{im_i})$.

Furthermore, two time thresholds $T_i^{\min}$ and $T_i^{\max}$ are pre-specified for each facility, where $T_i^{\min} < T_i^{\max}$. Denote by d_i and r_i the numbers of failures observed before $T_i^{\min}$ and $T_i^{\max}$, respectively. Let X_{ij} represent the j-th failure time corresponding to the i-th facility ($j = 1, 2, \ldots, m_i; i = 1, 2, \ldots, k$). According to the BIAPTIIHC scheme, the life test for each facility may terminate under one of the following three possible scenarios:

- Case I: If $X_{im_i} < T_i^{\min}$, the experiment concludes at the time of the m_i-th failure, i.e., at X_{im_i}. In this situation, the observed data correspond to the BPTIIC sample with m_i recorded failures.
- Case II: If $T_i^{\min} < X_{im_i} < T_i^{\max}$, the test also terminates at X_{im_i}. After the first d_i failures that occur prior to $T_i^{\min}$, no additional removals take place until the m_i-th failure, at which point all remaining test units are simultaneously withdrawn. The resulting dataset in this scenario represents the BAPTIIHC sample.
- Case III: If $T_i^{\min} < T_i^{\max} < X_{im_i}$, the experiment stops at the upper time limit $T_i^{\max}$. As in Case II, no units are removed after the initial d_i failures. At $T_i^{\max}$, all surviving units are withdrawn, and the number of observed failures in this case equals r_i.

Let $\mathcal{X}_i$ denote the IAPTIIHC failure-time sample obtained from the i-th group ($i = 1, 2, \ldots, k$), conducted under the corresponding progressive censoring plan $\mathcal{R}_i$, where

$$\mathcal{X}_i = \begin{cases} (X_{i1}, X_{i2}, \ldots, X_{im_i}), & \text{Case I,} \\ (X_{i1}, X_{i2}, \ldots, X_{im_i}), & \text{Case II,} \\ (X_{i1}, X_{i2}, \ldots, X_{ir_i}), & \text{Case III} \end{cases}$$

and

$$\mathcal{R}_i = \begin{cases} (R_{i1}, R_{i2}, \ldots, R_{im_i}), & \text{Case I,} \\ (R_{i1}, R_{i2}, \ldots, R_{id_i}, 0, \ldots, 0, R^*_{im_i}), & \text{Case II,} \\ (R_{i1}, R_{i2}, \ldots, R_{id_i}, 0, \ldots, 0, R^*_i), & \text{Case III,} \end{cases}$$

where $R_{im_i} = n_i - m_i - \sum_{j=1}^{m_i-1} R_{ij}$, $R^*_{im_i} = n_i - m_i - \sum_{j=1}^{d_i} R_{ij}$, and $R^*_i = n_i - r_i - \sum_{j=1}^{d_i} R_{ij}$.

Algorithm 1 presents the step-by-step implementation of the BIAPTIIHC scheme. Algorithm 1 clearly illustrates the operational structure of the proposed BIAPTIIHC scheme and its relationship with previously developed censoring mechanisms. In particular, Case I reduces to the classical BPTIIC structure, while Case II coincides with the BAPTIIHC scheme. Therefore, both schemes arise naturally as special cases of the proposed framework. The distinguishing feature of the BIAPTIIHC design lies in the incorporation of an additional upper time threshold, which guarantees termination within a controlled time horizon. This improvement addresses the potential drawback of prolonged test durations that may occur under BAPTIIHC schemes when highly reliable units are tested. By integrating block experimentation with adaptive and time-controlled termination rules, the BIAPTIIHC scheme achieves a balanced compromise between experimental efficiency and inferential accuracy. Consequently, it provides greater flexibility in practical reliability and survival studies, particularly when time constraints must be accommodated.

Algorithm 1 Algorithmic summary of the BIAPTIIHC scheme.

1: Specify the design parameters: sample size n_i, planned number of failures m_i, progressive censoring scheme $\mathcal{R}_i = (R_{i1}, \ldots, R_{im_i})$, and time thresholds $T_i^{\min} < T_i^{\max}$.
2: Begin the life test with n_i units.
3: Observe failures sequentially. At the j-th observed failure time X_{ij}:
- Remove R_{ij} surviving units if $X_{ij} < T_i^{\min}$.
- If $X_{ij} \geq T_i^{\min}$ and $j < m_i$, set subsequent removals to zero until termination.

4: Apply the termination rule:
- If $X_{im_i} < T_i^{\min}$, terminate at X_{im_i} (Case I).
- If $T_i^{\min} < X_{im_i} < T_i^{\max}$, terminate at X_{im_i} (Case II).
- If $X_{im_i} > T_i^{\max}$, terminate at $T_i^{\max}$ (Case III).

5: Record the observed failure times and the final removal configuration.

In the proposed BIAPTIIHC framework, and given the inherent similarities among the testing facilities in practical applications, it is reasonable to assume that the shape parameter β is common across all facilities. On the other hand, the DDTF can be characterized through facility-specific scale parameters δ_i ($i = 1, 2, \ldots, k$), where k denotes the total number of facilities in the BIAPTIIHC setup. Accordingly, the lifetimes of the units in the i-th facility are assumed to be independent and to follow the Weibull(δ_i, β) distribution. To assess the DDTF, previous studies have simply checked whether the interval estimates for δ_i overlap, without quantifying the extent of that overlap. To address this limitation, we introduce a new quantitative measure called the coverage similarity index (CSI), which reflects the percentage of overlap among the estimated intervals of the parameters δ_i across different facilities. This measure is discussed later in the simulation section.

When the variation among facilities is non-negligible, an overall population scale parameter δ can be obtained as a weighted average of the facility-specific parameters, given by

$$\delta = \frac{\sum_{i=1}^{k} \epsilon_i \delta_i}{\sum_{i=1}^{k} \epsilon_i}, \tag{2.6}$$

where ϵ_i represents a weight coefficient associated with the i-th facility obtained as $\epsilon_i = 1/\operatorname{Var}(\delta_i)$, where $\operatorname{Var}(\delta_i)$ is the variance associated with δ_i.

Now, let $\mathbf{x}_i$ denote the realization of $\mathcal{X}_i$ for $i = 1, 2, \ldots, k$. Then, the likelihood function (LF) corresponding to the i-th test group can be expressed as follows:

$$L_i(\delta_i, \beta; \mathbf{x}_i) = C_i \prod_{j=1}^{J_i} f(x_{ij}; \delta_i, \beta) \prod_{j=1}^{Q_i} \left[1 - F(x_{ij}; \delta_i, \beta)\right]^{R_{ij}} \left[1 - F(\tau_i; \delta_i, \beta)\right]^{R_i^\star},$$

where C_i is a constant that does not depend on the parameters,

$$(J_i, Q_i) = \begin{cases} (m_i, m_i - 1), & \text{Case I,} \\ (m_i, d_i), & \text{Case II,} \\ (r_i, d_i), & \text{Case III,} \end{cases} \quad \text{and} \quad (\tau_i, R_i^\star) = \begin{cases} (x_{im_i}, R_{im_i}), & \text{Case I,} \\ (x_{im_i}, R_{im_i}^*), & \text{Case II,} \\ (T_i^{\max}, R_i^*), & \text{Case III.} \end{cases}$$

Let $\mathbf{x} = (\mathbf{x}_1, \mathbf{x}_2, \ldots, \mathbf{x}_k)$, $\boldsymbol{\delta} = (\delta_1, \delta_2, \ldots, \delta_k)$, and then the LF of $\boldsymbol{\delta}$ and β with respect to the BIAPTIIHC data can be written as

$$\begin{aligned} L(\boldsymbol{\delta}, \beta; \mathbf{x}) &= \prod_{i=1}^{k} L_i(\delta_i, \beta; \mathbf{x}_i) \\ &= \prod_{i=1}^{k} \left\{ C_i \prod_{j=1}^{J_i} f(x_{ij}; \delta_i, \beta) \prod_{j=1}^{Q_i} \left[1 - F(x_{ij}; \delta_i, \beta)\right]^{R_{ij}} \left[1 - F(\tau_i; \delta_i, \beta)\right]^{R_i^\star} \right\}. \end{aligned} \tag{2.7}$$

3. Likelihood estimation

In this section, the ML estimation method is employed to estimate the model parameters and the associated RCs. Approximate confidence intervals (ACIs) are also constructed for all target parameters and RCs. Since the DDTF is characterized by variations in the scale parameters δ_i $(i = 1, 2, \ldots, k)$, the problem of estimating the DDTF is essentially reduced to estimating these δ_i values. In this study, the differences of interval estimates of δ_i $(i = 1, 2, \ldots, k)$ are regarded as measures of the DDTF. When such differences across facilities are found to be non-negligible, the overall scale parameter δ can be obtained using the weighted estimator of δ_i, as defined in (2.6).

3.1. Point estimation

Suppose that $\mathbf{x}$ denotes a BIAPTIIHC sample drawn from a Weibull population with a progressive removal pattern $\mathcal{R}_i$. By utilizing the PDF given in (2.1) and the CDF provided in (2.2), the full LF can be formulated using (2.7), without constant terms, as follows:

$$L(\boldsymbol{\delta}, \beta; \mathbf{x}) = \beta^{\sum_{i=1}^{k} J_i} \left(\prod_{i=1}^{k} \delta_i^{J_i} \right) \exp\left[(\beta - 1) \sum_{i=1}^{k} \sum_{j=1}^{J_i} \log(x_{ij}) - \sum_{i=1}^{k} \delta_i \varphi_i(\beta) \right], \tag{3.1}$$

where $\varphi_i(\beta) = \sum_{j=1}^{J_i} x_{ij}^{\beta} + \sum_{j=1}^{Q_i} R_{ij} x_{ij}^{\beta} + R_i^\star \tau_i^{\beta}$. The natural logarithm of the LF can be obtained from (3.1) as

$$\mathcal{L}(\boldsymbol{\delta}, \beta; \mathbf{x}) = \left(\sum_{i=1}^{k} J_i \right) \log(\beta) + \sum_{i=1}^{k} J_i \log(\delta_i) + (\beta - 1) \sum_{i=1}^{k} \sum_{j=1}^{J_i} \log(x_{ij}) - \sum_{i=1}^{k} \delta_i \varphi_i(\beta). \tag{3.2}$$

From (3.2), the MLEs of the unknown parameters $\boldsymbol{\delta}$ and β, denoted by $\hat{\boldsymbol{\delta}} = (\hat{\delta}_1, \hat{\delta}_2, \ldots, \hat{\delta}_k)$ and $\hat{\beta}$, can be obtained by solving the following normal equations:

$$\frac{\partial \mathcal{L}(\boldsymbol{\delta}, \beta; \mathbf{x})}{\partial \delta_i} = \frac{J_i}{\delta_i} - \varphi_i(\beta) = 0 \tag{3.3}$$

and

$$\frac{\partial \mathcal{L}(\boldsymbol{\delta}, \beta; \mathbf{x})}{\partial \beta} = \frac{\sum_{i=1}^{k} J_i}{\beta} + \sum_{i=1}^{k} \sum_{j=1}^{J_i} \log(x_{ij}) - \sum_{i=1}^{k} \delta_i \varphi_i'(\beta) = 0, \tag{3.4}$$

where $\varphi_i^{'}(\beta) = \sum_{j=1}^{J_i} x_{ij}^{\beta}\log(x_{ij}) + \sum_{j=1}^{Q_i} R_{ij}x_{ij}^{\beta}\log(x_{ij}) + R_i^{\star}\tau_i^{\beta}\log(\tau_i)$. Based on the normal equation in (3.3), the MLE of δ_i can be acquired as a function of the shape parameter β, as

$$\hat{\delta}_i(\beta) = \frac{J_i}{\varphi_i(\beta)},\ i = 1,\ldots,k. \tag{3.5}$$

By substituting $\widehat{\delta_i}(\beta)$ from (3.5) into (3.4), the following equation for β is obtained:

$$\frac{\sum_{i=1}^{k} J_i}{\beta} + \sum_{i=1}^{k}\sum_{j=1}^{J_i}\log(x_{ij}) - \sum_{i=1}^{k} J_i\frac{\varphi_i^{'}\beta)}{\varphi_i(\beta)} = 0. \tag{3.6}$$

Using (3.6), the MLE of β is determined iteratively as the fixed point of the function $\xi(\beta) = \beta$, where

$$\xi(\beta) = \left[\frac{\sum_{i=1}^{k} J_i\frac{\varphi_i^{'}(\beta)}{\varphi_i(\beta)} - \sum_{i=1}^{k}\sum_{j=1}^{J_i}\log(x_{ij})}{\sum_{i=1}^{k} J_i}\right]^{-1}.$$

Accordingly, the MLE of β can be carried out using $\beta^{(l+1)} = \xi(\beta^{(l)})$, where $\beta^{(l)}$ represents the estimate of β at the l-th iteration. The iterative process is repeated until convergence, which is achieved when $\left|\beta^{(l+1)} - \beta^{(l)}\right| < \varepsilon$, where ε is a small positive constant that specifies the convergence tolerance. Once the MLE of β is acquired, the MLE of δ_i is subsequently obtained from (3.5) as $\hat{\delta}_i(\hat{\beta})$.

By employing the invariance property of the MLEs, the MLEs of the RCs can be obtained by substituting the true parameter values with their corresponding MLEs. As a result, the MLEs of the RF, HRF, and MTTF can be directly derived from (2.3)–(2.5), respectively, as follows:

$$\hat{R}(x) = e^{-\hat{\delta}x^{\hat{\beta}}},\quad \hat{H}(x) = \hat{\delta}\hat{\beta}x^{\hat{\beta}-1},$$

and

$$\hat{\mu} = \frac{\Gamma\left(1+\frac{1}{\hat{\beta}}\right)}{\hat{\delta}^{1/\hat{\beta}}},$$

where $\hat{\delta}$ can be obtained from (2.6) as follows:

$$\hat{\delta} = \frac{\sum_{i=1}^{k}\hat{\epsilon}_i\hat{\delta}_i}{\sum_{i=1}^{k}\hat{\epsilon}_i},$$

where $\hat{\epsilon}_i = 1/\widehat{\mathrm{Var}}(\hat{\delta}_i)$, and $\widehat{\mathrm{Var}}(\hat{\delta}_i)$ is the estimated variance of the MLE $\hat{\delta}_i$ discussed in the next subsection.

3.2. Interval estimation

As noted by Zhu [20], the DDTF can be evaluated using the differences between the interval estimates of δ_i. To achieve this, we construct ACIs for the scale parameters δ_i ($i = 1,\ldots,k$), as well as for the shape parameter β, the RCs, and the combined parameter δ. The ACIs are derived based on the large-sample approximation theory. According to the asymptotic normality property of the MLEs, we have $(\hat{\boldsymbol{\delta}},\hat{\beta}) \sim N_{k+1}\left[(\boldsymbol{\delta},\beta), \boldsymbol{I}^{-1}(\boldsymbol{\delta},\beta)\right]$, where $\boldsymbol{I}^{-1}(\boldsymbol{\delta},\beta)$ denotes the variance–covariance matrix of the

estimators. In practice, this matrix is estimated by substituting the MLEs of the parameters, that is, $\boldsymbol{I}^{-1}(\hat{\boldsymbol{\delta}}, \hat{\beta})$, which is obtained through the inversion of the observed Fisher information matrix, as follows:

$$\boldsymbol{I}^{-1}(\hat{\boldsymbol{\delta}}, \hat{\beta}) = -\begin{bmatrix} \frac{\partial^2 \mathcal{L}(\boldsymbol{\delta}, \beta; \mathbf{x})}{\partial \delta_1^2} & \frac{\partial^2 \mathcal{L}(\boldsymbol{\delta}, \beta; \mathbf{x})}{\partial \delta_1 \partial \delta_2} & \cdots & \frac{\partial^2 \mathcal{L}(\boldsymbol{\delta}, \beta; \mathbf{x})}{\partial \delta_1 \partial \delta_k} & \frac{\partial^2 \mathcal{L}(\boldsymbol{\delta}, \beta; \mathbf{x})}{\partial \delta_1 \partial \beta} \\ \frac{\partial^2 \mathcal{L}(\boldsymbol{\delta}, \beta; \mathbf{x})}{\partial \delta_2 \partial \delta_1} & \frac{\partial^2 \mathcal{L}(\boldsymbol{\delta}, \beta; \mathbf{x})}{\partial \delta_2^2} & \cdots & \frac{\partial^2 \mathcal{L}(\boldsymbol{\delta}, \beta; \mathbf{x})}{\partial \delta_2 \partial \delta_k} & \frac{\partial^2 \mathcal{L}(\boldsymbol{\delta}, \beta; \mathbf{x})}{\partial \delta_2 \partial \beta} \\ \vdots & \vdots & \ddots & \vdots & \vdots \\ \frac{\partial^2 \mathcal{L}(\boldsymbol{\delta}, \beta; \mathbf{x})}{\partial \delta_k \partial \delta_1} & \frac{\partial^2 \mathcal{L}(\boldsymbol{\delta}, \beta; \mathbf{x})}{\partial \delta_k \partial \delta_2} & \cdots & \frac{\partial^2 \mathcal{L}(\boldsymbol{\delta}, \beta; \mathbf{x})}{\partial \delta_k^2} & \frac{\partial^2 \mathcal{L}(\boldsymbol{\delta}, \beta; \mathbf{x})}{\partial \delta_k \partial \beta} \\ \frac{\partial^2 \mathcal{L}(\boldsymbol{\delta}, \beta; \mathbf{x})}{\partial \beta \partial \delta_1} & \frac{\partial^2 \mathcal{L}(\boldsymbol{\delta}, \beta; \mathbf{x})}{\partial \beta \partial \delta_2} & \cdots & \frac{\partial^2 \mathcal{L}(\boldsymbol{\delta}, \beta; \mathbf{x})}{\partial \beta \partial \delta_k} & \frac{\partial^2 \mathcal{L}(\boldsymbol{\delta}, \beta; \mathbf{x})}{\partial \beta^2} \end{bmatrix}^{-1}_{(\boldsymbol{\delta}, \beta) = (\hat{\boldsymbol{\delta}}, \hat{\beta})}, \tag{3.7}$$

where the second derivatives are given by

$$\frac{\partial^2 \mathcal{L}(\boldsymbol{\delta}, \beta; \mathbf{x})}{\partial \delta_i^2} = -\frac{J_i}{\delta_i^2}, \ \frac{\partial^2 \mathcal{L}(\boldsymbol{\delta}, \beta; \mathbf{x})}{\partial \delta_i \partial \delta_l} = 0, \ i, l = 1, 2, \ldots, k, \ i \neq l,$$

$$\frac{\partial^2 \mathcal{L}(\boldsymbol{\delta}, \beta; \mathbf{x})}{\partial \beta^2} = -\frac{\sum_{i=1}^{k} J_i}{\beta^2} - \sum_{i=1}^{k} \delta_i \varphi_i^{''}(\beta), \text{ and } \frac{\partial^2 \mathcal{L}(\boldsymbol{\delta}, \beta; \mathbf{x})}{\partial \delta_i \partial \beta} = -\varphi_i^{'}(\beta),$$

where $\varphi_i^{''}(\beta) = \sum_{j=1}^{J_i} x_{ij}^{\beta} \log^2(x_{ij}) + \sum_{j=1}^{Q_i} R_{ij} x_{ij}^{\beta} \log^2(x_{ij}) + R_i^{\star} \tau_i^{\beta} \log^2(\tau_i)$. Since the estimated variance–covariance matrix is symmetric, the matrix in (3.7) can be equivalently represented in a simplified form as follows:

$$\boldsymbol{I}^{-1}(\hat{\boldsymbol{\delta}}, \hat{\beta}) = \begin{bmatrix} \widehat{\mathrm{Var}}(\hat{\delta}_1) & 0 & \cdots & 0 & \widehat{\mathrm{Cov}}(\hat{\delta}_1, \hat{\beta}) \\ & \widehat{\mathrm{Var}}(\hat{\delta}_2) & \cdots & 0 & \widehat{\mathrm{Cov}}(\hat{\delta}_2, \hat{\beta}) \\ & & \ddots & \vdots & \vdots \\ & & & \widehat{\mathrm{Var}}(\hat{\delta}_k) & \widehat{\mathrm{Cov}}(\hat{\delta}_k, \hat{\beta}) \\ & & & & \widehat{\mathrm{Var}}(\hat{\beta}) \end{bmatrix}.$$

For any $0 < \alpha < 1$, the $100(1-\alpha)\%$ ACIs for δ_i $(i = 1, 2, \ldots, k)$ and β can be constructed, respectively, as follows:

$$\left(\hat{\delta}_i - z_{\alpha/2} \sqrt{\widehat{\mathrm{Var}}(\hat{\delta}_i)}, \ \hat{\delta}_i + z_{\alpha/2} \sqrt{\widehat{\mathrm{Var}}(\hat{\delta}_i)}\right)$$

and

$$\left(\hat{\beta} - z_{\alpha/2} \sqrt{\widehat{\mathrm{Var}}(\hat{\beta})}, \ \hat{\beta} + z_{\alpha/2} \sqrt{\widehat{\mathrm{Var}}(\hat{\beta})}\right),$$

where $z_{\alpha/2}$ denotes the quantile of the standard normal distribution such that $P(Z > z_{\alpha/2}) = \alpha/2$, with $Z \sim N(0, 1)$.

On the other hand, to construct the ACIs for the parameter δ and the RCs, we employ the delta method to approximate the variances of $\hat{\delta}$, $\hat{R}(x)$, $\hat{H}(x)$, and the MLE of the MTTF $\hat{\mu}$. To implement this approach, it is first necessary to derive the corresponding gradient vectors for each of these quantities, as presented below:

$$\boldsymbol{\Delta}_\delta = \zeta \begin{pmatrix} \epsilon_1 \\ \epsilon_2 \\ \vdots \\ \epsilon_k \\ 0 \end{pmatrix}, \quad \boldsymbol{\Delta}_R = -R(x)\,\zeta\, x^\beta \begin{pmatrix} \epsilon_1 \\ \epsilon_2 \\ \vdots \\ \epsilon_k \\ \delta \log(x)/\zeta \end{pmatrix},$$

$$\boldsymbol{\Delta}_H = \zeta\beta x^{\beta-1} \begin{pmatrix} \epsilon_1 \\ \epsilon_2 \\ \vdots \\ \epsilon_k \\ \delta x^*/\zeta\beta \end{pmatrix}, \quad \text{and} \quad \boldsymbol{\Delta}_\mu = -\frac{\mu\zeta}{\beta\delta} \begin{pmatrix} \epsilon_1 \\ \epsilon_2 \\ \vdots \\ \epsilon_k \\ \delta\psi^*/\zeta\beta^2 \end{pmatrix},$$

where $\zeta = 1/\sum_{i=1}^{k} \epsilon_i$, $x^* = 1 + \beta \log(x)$, $\psi^* = \psi(1 + 1/\beta) - \log(\delta)$, where $\psi(.)$ is the digamma function. Accordingly, the estimated variances of $\hat{\delta}$, $\hat{R}(x)$, $\hat{H}(x)$, and $\hat{\mu}$ can be approximated, respectively, as follows:

$$\widehat{\mathrm{Var}}(\hat{\delta}) \approx \left[\boldsymbol{\Delta}_\delta^\top \boldsymbol{I}^{-1}(\hat{\boldsymbol{\delta}}, \hat{\beta})\boldsymbol{\Delta}_\delta\right]\Big|_{(\boldsymbol{\delta},\beta)=(\hat{\boldsymbol{\delta}},\hat{\beta})}, \quad \widehat{\mathrm{Var}}(\hat{R}(x)) \approx \left[\boldsymbol{\Delta}_R^\top \boldsymbol{I}^{-1}(\hat{\boldsymbol{\delta}}, \hat{\beta})\boldsymbol{\Delta}_R\right]\Big|_{(\boldsymbol{\delta},\beta)=(\hat{\boldsymbol{\delta}},\hat{\beta})},$$

$$\widehat{\mathrm{Var}}(\hat{H}(x)) \approx \left[\boldsymbol{\Delta}_H^\top \boldsymbol{I}^{-1}(\hat{\boldsymbol{\delta}}, \hat{\beta})\boldsymbol{\Delta}_H\right]\Big|_{(\boldsymbol{\delta},\beta)=(\hat{\boldsymbol{\delta}},\hat{\beta})}, \quad \text{and} \quad \widehat{\mathrm{Var}}(\hat{\mu}) \approx \left[\boldsymbol{\Delta}_\mu^\top \boldsymbol{I}^{-1}(\hat{\boldsymbol{\delta}}, \hat{\beta})\boldsymbol{\Delta}_\mu\right]\Big|_{(\boldsymbol{\delta},\beta)=(\hat{\boldsymbol{\delta}},\hat{\beta})}.$$

Therefore, the $100(1-\alpha)\%$ ACIs for δ, and the RCs $R(x)$, $H(x)$, and μ can be obtained, respectively, as

$$\left(\hat{\delta} - z_{\alpha/2}\sqrt{\widehat{\mathrm{Var}}(\hat{\delta})},\ \hat{\delta} + z_{\alpha/2}\sqrt{\widehat{\mathrm{Var}}(\hat{\delta})}\right),$$

$$\left(\hat{R}(x) - z_{\alpha/2}\sqrt{\widehat{\mathrm{Var}}(\hat{R}(x))},\ \hat{R}(x) + z_{\alpha/2}\sqrt{\widehat{\mathrm{Var}}(\hat{R}(x))}\right),$$

$$\left(\hat{H}(x) - z_{\alpha/2}\sqrt{\widehat{\mathrm{Var}}(\hat{H}(x))},\ \hat{H}(x) + z_{\alpha/2}\sqrt{\widehat{\mathrm{Var}}(\hat{H}(x))}\right),$$

and

$$\left(\hat{\mu} - z_{\alpha/2}\sqrt{\widehat{\mathrm{Var}}(\hat{\mu})},\ \hat{\mu} + z_{\alpha/2}\sqrt{\widehat{\mathrm{Var}}(\hat{\mu})}\right).$$

4. Product of spacings estimation

In this section, the MPS estimation method is employed to estimate the model parameters and the associated RCs under the BIAPTIIHC scheme. Originally introduced by Cheng and Amin [36], the MPS method provides a powerful and reliable alternative to the traditional ML estimation method, particularly in cases where the likelihood function is highly nonlinear, multimodal, or suffers from numerical instability. The MPS method is founded on maximizing the geometric mean of the spacings between successive cumulative probabilities of ordered observations. This approach yields estimators

that retain many of the desirable large-sample properties of MLEs, such as consistency and asymptotic efficiency, as shown by Cheng and Amin [36]. Subsequent theoretical advancements were made by Ghosh and Jammalamadaka [37] and Anatolyev and Kosenok [38], who investigated the asymptotic distributional behavior and invariance properties of the MPS estimators (MPSEs). In recent years, the MPS estimation method has been successfully applied in a wide range of statistical modeling contexts. Examples include Singh et al. [39], Volovskiy and Kamps [40], and Khan et al. [41], among others.

Based on an BIAPTIIHC sample, let $\mathcal{D}_{ij} = F(x_{ij};\delta_i,\beta) - F(x_{ij^*};\delta_i,\beta)$, where $j^* = j-1, i = 1,\ldots,k, j = 1,\ldots,J_i$, with $F(x_{i0};\delta_i,\beta) = 0$ and $F(x_{iJ_i+1};\delta_i,\beta) = 1$. Then, the spacings function (SF) of $\boldsymbol{\delta}$ and β with respect to the BIAPTIIHC data can be expressed as

$$S(\boldsymbol{\delta},\beta;\mathbf{x}) = \prod_{i=1}^{k}\left\{C_i\prod_{j=1}^{J_i+1}\mathcal{D}_{ij}\prod_{j=1}^{Q_i}\left[1-F(x_{ij};\delta_i,\beta)\right]^{R_{ij}}\left[1-F(\tau_i;\delta_i,\beta)\right]^{R_i^\star}\right\}. \tag{4.1}$$

4.1. Point estimation

Suppose that $\mathbf{x}$ represents a BIAPTIIHC sample obtained from a Weibull population under the progressive removal scheme $\mathcal{R}_i$. Using the CDF defined in (2.2), the full SF, excluding constant terms, can be expressed based on (4.1) as follows:

$$S(\boldsymbol{\delta},\beta;\mathbf{x}) = \exp\left[\sum_{i=1}^{k}\vartheta_i(\delta_i,\beta) - \sum_{i=1}^{k}\delta_i\varphi_i(\beta)\right], \tag{4.2}$$

where $\vartheta_i(\delta_i,\beta) = \sum_{j=1}^{J_i}\log\left(1-e^{-\delta_i(x_{ij}^\beta - x_{ij^*}^\beta)}\right)$. The natural logarithm of (4.2) follows:

$$\mathcal{S}(\boldsymbol{\delta},\beta;\mathbf{x}) = \sum_{i=1}^{k}\vartheta_i(\delta_i,\beta) - \sum_{i=1}^{k}\delta_i\varphi_i(\beta). \tag{4.3}$$

The MPSEs of δ_i and β can be acquired by maximizing (4.3) with respect to these unknown parameters, or equivalently solving the following normal equations simultaneously

$$\frac{\partial\mathcal{S}(\boldsymbol{\delta},\beta;\mathbf{x})}{\partial\delta_i} = -\sum_{j=1}^{J_i}\frac{v_{ij}}{1-e^{\delta_i v_{ij}}} - \varphi_i(\beta) = 0, \quad i = 1,\ldots,k, \tag{4.4}$$

and

$$\frac{\partial\mathcal{S}(\boldsymbol{\delta},\beta;\mathbf{x})}{\partial\beta} = -\sum_{i=1}^{k}\sum_{j=1}^{J_i}\frac{\delta_i u_{ij}}{1-e^{\delta_i v_{ij}}} - \sum_{i=1}^{k}\varphi_i'(\beta) = 0, \tag{4.5}$$

where $v_{ij} \equiv v_{ij}(x_{ij};\delta_i,\beta) = x_{ij}^\beta - x_{ij^*}^\beta$ and $u_{ij} \equiv u_{ij}(x_{ij};\delta_i,\beta) = x_{ij}^\beta\log(x_{ij}) - x_{ij^*}^\beta\log(x_{ij^*})$.

The system of nonlinear equations given in (4.4) must be solved simultaneously to obtain the MPSEs of the model parameters δ_i and β, denoted by $\tilde{\delta}_i$ and $\tilde{\beta}$, respectively. Due to the high degree of nonlinearity in these equations, closed-form analytical solutions are not available. Consequently, numerical optimization algorithms such as the Newton–Raphson method are utilized to obtain the

MPSEs efficiently. Once the estimates $\tilde{\delta}_i$ and $\tilde{\beta}$ are obtained, the invariance property of the MPSEs can be applied to derive the corresponding estimates of the RCs and the common parameter δ as follows:

$$\tilde{R}(x) = e^{-\tilde{\delta}x^{\tilde{\beta}}}, \quad \tilde{H}(x) = \tilde{\delta}\tilde{\beta}x^{\tilde{\beta}-1},$$

and

$$\tilde{\mu} = \frac{\Gamma\left(1+\frac{1}{\tilde{\beta}}\right)}{\tilde{\delta}^{1/\tilde{\beta}}},$$

where $\tilde{\delta}$ can be acquired using (2.6) as

$$\tilde{\delta} = \frac{\sum_{i=1}^{k}\tilde{\epsilon}_i\tilde{\delta}_i}{\sum_{i=1}^{k}\tilde{\epsilon}_i},$$

where $\tilde{\epsilon}_i = 1/\widetilde{\mathrm{Var}}(\tilde{\delta}_i)$, and $\widetilde{\mathrm{Var}}(\tilde{\delta}_i)$ is the estimated variance of the MPSE $\tilde{\delta}_i$, which will be discussed in the following subsection.

4.2. Interval estimation

As discussed in the preceding section, the differences between the interval estimates of δ_i are utilized to evaluate the DDTF. This can be accomplished by constructing the ACIs of δ_i based on the asymptotic normality of the MPSEs. In addition to these intervals, we also derive ACIs for the shape parameter β, the RCs, and the common scale parameter δ. According to the asymptotic normality property of the MPSEs, we have $(\tilde{\boldsymbol{\delta}},\tilde{\beta}) \sim N_{k+1}\left[(\boldsymbol{\delta},\beta), \boldsymbol{\Sigma}^{-1}(\boldsymbol{\delta},\beta)\right]$, where $\boldsymbol{\Sigma}^{-1}(\boldsymbol{\delta},\beta)$ represents the variance–covariance matrix of the estimators. Here, we estimate this matrix using the MPSEs of the parameters, yielding $\boldsymbol{\Sigma}^{-1}(\tilde{\boldsymbol{\delta}},\tilde{\beta})$, which can be expressed as follows:

$$\boldsymbol{\Sigma}^{-1}(\tilde{\boldsymbol{\delta}},\tilde{\beta}) = -\begin{bmatrix} \frac{\partial^2\mathcal{S}(\boldsymbol{\delta},\beta;\mathbf{x})}{\partial\delta_1^2} & \frac{\partial^2\mathcal{S}(\boldsymbol{\delta},\beta;\mathbf{x})}{\partial\delta_1\partial\delta_2} & \cdots & \frac{\partial^2\mathcal{S}(\boldsymbol{\delta},\beta;\mathbf{x})}{\partial\delta_1\partial\delta_k} & \frac{\partial^2\mathcal{S}(\boldsymbol{\delta},\beta;\mathbf{x})}{\partial\delta_1\partial\beta} \\ \frac{\partial^2\mathcal{S}(\boldsymbol{\delta},\beta;\mathbf{x})}{\partial\delta_2\partial\delta_1} & \frac{\partial^2\mathcal{S}(\boldsymbol{\delta},\beta;\mathbf{x})}{\partial\delta_2^2} & \cdots & \frac{\partial^2\mathcal{S}(\boldsymbol{\delta},\beta;\mathbf{x})}{\partial\delta_2\partial\delta_k} & \frac{\partial^2\mathcal{S}(\boldsymbol{\delta},\beta;\mathbf{x})}{\partial\delta_2\partial\beta} \\ \vdots & \vdots & \ddots & \vdots & \vdots \\ \frac{\partial^2\mathcal{S}(\boldsymbol{\delta},\beta;\mathbf{x})}{\partial\delta_k\partial\delta_1} & \frac{\partial^2\mathcal{S}(\boldsymbol{\delta},\beta;\mathbf{x})}{\partial\delta_k\partial\delta_2} & \cdots & \frac{\partial^2\mathcal{S}(\boldsymbol{\delta},\beta;\mathbf{x})}{\partial\delta_k^2} & \frac{\partial^2\mathcal{S}(\boldsymbol{\delta},\beta;\mathbf{x})}{\partial\delta_k\partial\beta} \\ \frac{\partial^2\mathcal{S}(\boldsymbol{\delta},\beta;\mathbf{x})}{\partial\beta\partial\delta_1} & \frac{\partial^2\mathcal{S}(\boldsymbol{\delta},\beta;\mathbf{x})}{\partial\beta\partial\delta_2} & \cdots & \frac{\partial^2\mathcal{S}(\boldsymbol{\delta},\beta;\mathbf{x})}{\partial\beta\partial\delta_k} & \frac{\partial^2\mathcal{S}(\boldsymbol{\delta},\beta;\mathbf{x})}{\partial\beta^2} \end{bmatrix}^{-1}_{(\boldsymbol{\delta},\beta)=(\tilde{\boldsymbol{\delta}},\tilde{\beta})}, \tag{4.6}$$

where

$$\frac{\partial^2\mathcal{S}(\boldsymbol{\delta},\beta;\mathbf{x})}{\partial\delta_i^2} = -\sum_{j=1}^{J_i}\frac{v_{ij}^2e^{\delta_iv_{ij}}}{\left(1-e^{\delta_iv_{ij}}\right)^2}, \quad \frac{\partial^2\mathcal{S}(\boldsymbol{\delta},\beta;\mathbf{x})}{\partial\delta_i\partial\delta_l} = 0, i,l = 1,\ldots,k, \quad i \neq l,$$

$$\frac{\partial^2\mathcal{S}(\boldsymbol{\delta},\beta;\mathbf{x})}{\partial\beta^2} = -\sum_{i=1}^{k}\sum_{j=1}^{J_i}\frac{\delta_ic_{ij}}{1-e^{\delta_iv_{ij}}} - \sum_{i=1}^{k}\sum_{j=1}^{J_i}\frac{\delta_i^2u_{ij}^2e^{\delta_iv_{ij}}}{\left(1-e^{\delta_iv_{ij}}\right)^2} - \sum_{i=1}^{k}\varphi_i^{''}(\beta),$$

and

$$\frac{\partial^2 \mathcal{S}(\boldsymbol{\delta},\beta;\mathbf{x})}{\partial\delta_i\partial\beta} = \sum_{j=1}^{J_i} \frac{u_{ij}\left(e^{\delta_i v_{ij}} - 1 - \delta_i v_{ij} e^{\delta_i v_{ij}}\right)}{\left(1-e^{\delta_i v_{ij}}\right)^2} - \varphi_i^{'}(\beta),$$

where $c_{ij} \equiv c_{ij}(x_{ij};\delta_i,\beta) = x_{ij}^{\beta}\log^2(x_{ij}) - x_{ij^*}^{\beta}\log^2(x_{ij^*})$. Thus, we can simply write the matrix in (4.6) as follows:

$$\boldsymbol{\Sigma}^{-1}(\tilde{\boldsymbol{\delta}},\tilde{\beta}) = \begin{bmatrix} \widetilde{\mathrm{Var}}(\tilde{\delta}_1) & 0 & \cdots & 0 & \widetilde{\mathrm{Cov}}(\tilde{\delta}_1,\tilde{\beta}) \\ & \widetilde{\mathrm{Var}}(\tilde{\delta}_2) & \cdots & 0 & \widetilde{\mathrm{Cov}}(\tilde{\delta}_2,\tilde{\beta}) \\ & & \ddots & \vdots & \vdots \\ & & & \widetilde{\mathrm{Var}}(\tilde{\delta}_k) & \widetilde{\mathrm{Cov}}(\tilde{\delta}_k,\tilde{\beta}) \\ & & & & \widetilde{\mathrm{Var}}(\tilde{\beta}) \end{bmatrix}.$$

Therefore, the $100(1-\alpha)\%$ ACIs based on the MPSEs for δ_i $(i = 1, 2, \ldots, k)$ and β can be computed, respectively, as

$$\left(\tilde{\delta}_i - z_{\alpha/2}\sqrt{\widetilde{\mathrm{Var}}(\tilde{\delta}_i)},\ \tilde{\delta}_i + z_{\alpha/2}\sqrt{\widetilde{\mathrm{Var}}(\tilde{\delta}_i)}\right)$$

and

$$\left(\tilde{\beta} - z_{\alpha/2}\sqrt{\widetilde{\mathrm{Var}}(\tilde{\beta})},\ \tilde{\beta} + z_{\alpha/2}\sqrt{\widetilde{\mathrm{Var}}(\tilde{\beta})}\right).$$

On the other hand, by employing the delta method and the acquired MPSEs of $\delta_i, i = 1, \ldots, k$, and β, we can approximate the estimated variances of the MPSEs $\tilde{\delta}$, $\tilde{R}(x)$, $\tilde{H}(x)$, and $\tilde{\mu}$, respectively, as

$$\widetilde{\mathrm{Var}}(\tilde{\delta}) \approx \left[\boldsymbol{\Delta}_{\delta}^{\top}\boldsymbol{\Sigma}^{-1}(\tilde{\boldsymbol{\delta}},\tilde{\beta})\boldsymbol{\Delta}_{\delta}\right]\Big|_{(\boldsymbol{\delta},\beta)=(\tilde{\boldsymbol{\delta}},\tilde{\beta})},\quad \widetilde{\mathrm{Var}}(\tilde{R}(x)) \approx \left[\boldsymbol{\Delta}_{R}^{\top}\boldsymbol{\Sigma}^{-1}(\tilde{\boldsymbol{\delta}},\tilde{\beta})\boldsymbol{\Delta}_{R}\right]\Big|_{(\boldsymbol{\delta},\beta)=(\tilde{\boldsymbol{\delta}},\tilde{\beta})},$$

$$\widetilde{\mathrm{Var}}(\tilde{H}(x)) \approx \left[\boldsymbol{\Delta}_{\delta}^{\top}\boldsymbol{\Sigma}^{-1}(\tilde{\boldsymbol{\delta}},\tilde{\beta})\boldsymbol{\Delta}_{H}\right]\Big|_{(\boldsymbol{\delta},\beta)=(\tilde{\boldsymbol{\delta}},\tilde{\beta})},\quad \text{and}\quad \widetilde{\mathrm{Var}}(\tilde{\mu}) \approx \left[\boldsymbol{\Delta}_{\mu}^{\top}\boldsymbol{\Sigma}^{-1}(\tilde{\boldsymbol{\delta}},\tilde{\beta})\boldsymbol{\Delta}_{\mu}\right]\Big|_{(\boldsymbol{\delta},\beta)=(\tilde{\boldsymbol{\delta}},\tilde{\beta})}.$$

Accordingly, the $100(1-\alpha)\%$ ACIs for δ, and the RCs can be computed as

$$\left(\tilde{\delta} - z_{\alpha/2}\sqrt{\widetilde{\mathrm{Var}}(\tilde{\delta})},\ \tilde{\delta} + z_{\alpha/2}\sqrt{\widetilde{\mathrm{Var}}(\tilde{\delta})}\right),$$

$$\left(\tilde{R}(x) - z_{\alpha/2}\sqrt{\widetilde{\mathrm{Var}}(\tilde{R}(x))},\ \tilde{R}(x) + z_{\alpha/2}\sqrt{\widetilde{\mathrm{Var}}(\tilde{R}(x))}\right),$$

$$\left(\tilde{H}(x) - z_{\alpha/2}\sqrt{\widetilde{\mathrm{Var}}(\tilde{H}(x))},\ \tilde{H}(x) + z_{\alpha/2}\sqrt{\widetilde{\mathrm{Var}}(\tilde{H}(x))}\right),$$

and

$$\left(\tilde{\mu} - z_{\alpha/2}\sqrt{\widetilde{\mathrm{Var}}(\tilde{\mu})},\ \tilde{\mu} + z_{\alpha/2}\sqrt{\widetilde{\mathrm{Var}}(\tilde{\mu})}\right).$$

5. Simulation study

In this section, a simulation study is conducted to compare the efficiency of various point and interval estimators of the Weibull parameters, the RCs, and the DDTF under the BIAPTIIHC sampling scheme. The true values of the model parameters are set to $(\delta, \beta) = (0.6, 1.5)$, and the RF and HRF are evaluated at mission time one in all cases. The parameter values are selected to represent a moderate-scale Weibull distribution with an increasing hazard rate, which is commonly encountered in reliability and survival applications. This choice allows assessment of estimator performance under a non-trivial hazard structure while avoiding extreme parameter settings. Different scenarios are considered for the number of facilities k, the sample sizes and numbers of failures (n_i, m_i), the threshold times $(T_i^{\min}, T_i^{\max})$, and the censoring schemes (CSs). Table 1 presents the various configurations of k and (n_i, m_i). In all scenarios, two sets of thresholds are examined, namely, $(T_i^{\min}, T_i^{\max}) = (1, 1.5)$ and $(1.25, 2)$ for $i = 1, \ldots, k$. Similarly, the selected threshold values $(T_i^{\min}, T_i^{\max})$ were chosen to represent moderate and relatively extended termination windows, allowing investigation of how time constraints influence estimation accuracy under the proposed design. Furthermore, two different censoring schemes are applied under the various facilities, as described below.

- CS-I: $\mathcal{R}_i = ((n_i - m_i), 0 * (m_i - 1)), i = 1, \ldots, k.$
- CS-II: $\mathcal{R}_i = (n_i - m_i)/m_i, i = 1, \ldots, k,$

where $0 * (m_i - 1)$ means 0 repeated $(m_i - 1)$ times. The two censoring schemes were chosen to reflect distinct practical scenarios. CS-I corresponds to a highly front-loaded removal structure, where most surviving units are withdrawn at the first failure, representing aggressive progressive censoring. In contrast, CS-II distributes removals more evenly across failure times, reflecting a more gradual censoring process. Comparing these schemes enables evaluation of estimator sensitivity to different censoring intensities and removal patterns.

Table 1. Various scenarios for simulation study.

k	$N = (n_1, n_2, \ldots, n_k)$	$M = (m_1, m_2, \ldots, m_k)$
3	$N_1 = (30, 40, 60)$	$M_1 = (5, 10, 10)$
		$M_2 = (10, 10, 15)$
4	$N_2 = (40, 50, 60, 80)$	$M_3 = (5, 10, 15, 20)$
		$M_4 = (20, 25, 30, 40)$

For each of the sixteen scenarios, 1000 BIAPTIIHC samples are generated, and all computations are performed using the *RStudio* software platform. To assess the performance of the point estimators, namely, the MLEs and MPSEs, both the average absolute bias and the average mean squared error (MSE) are computed. For the interval estimators, based on the ACIs derived from the MLEs and MPSEs, the average interval length (AIL) and the coverage probability (CP) are used as evaluation criteria. The corresponding results are summarized in Tables 2–5.

Table 2. The point and interval results for $k = 3$ and CS-I.

(N, M)	(T_i^{min}, T_i^{max})	Par	MLE		MPSE	
			Bias(MSE)	AIL(CP)	Bias(MSE)	AIL(CP)
(N_1, M_1)	$(1, 1.5)$	δ_1	0.1145(0.2362)	2.2619(95.3)	0.0020(0.1022)	2.2794(98.8)
		δ_2	0.0404(0.0532)	1.6067(98.6)	0.0016(0.0375)	1.6110(99.5)
		δ_3	0.0591(0.0570)	1.5899(98.2)	0.0098(0.0396)	1.6029(99.3)
		β	0.0425(0.0668)	0.6353(80.1)	0.2372(0.1040)	0.6774(82.2)
		δ	0.0982(0.0399)	0.9927(96.8)	0.0320(0.0202)	0.9997(99.5)
		$R(x)$	0.0489(0.0103)	0.5574(93.0)	0.0136(0.0064)	0.6035(98.7)
		$H(x)$	0.1744(0.1316)	1.5922(96.5)	0.0743(0.0550)	1.3838(99.5)
		μ	0.0885(0.1036)	1.8176(87.2)	0.2754(0.4837)	3.3400(98.1)
	$(1.25, 2)$	δ_1	0.1280(0.2150)	2.0398(94.7)	0.0340(0.0926)	2.0455(97.9)
		δ_2	0.0351(0.0433)	1.4462(98.1)	0.0183(0.0316)	1.4338(99.2)
		δ_3	0.0430(0.0479)	1.4452(98.4)	0.0179(0.0336)	1.4358(99.5)
		β	0.0435(0.0558)	0.5697(81.0)	0.2107(0.0838)	0.5964(83.9)
		δ	0.0807(0.0305)	0.9042(96.9)	0.0386(0.0163)	0.9003(99.6)
		$R(x)$	0.0807(0.0305)	0.9042(96.9)	0.0386(0.0163)	0.9003(99.6)
		$H(x)$	0.1446(0.0964)	1.3951(96.1)	0.0557(0.0397)	1.1987(99.8)
		μ	0.0853(0.0711)	1.6860(89.8)	0.1627(0.1610)	2.5168(97.8)
(N_1, M_2)	$(1, 1.5)$	δ_1	0.0307(0.0601)	1.6230(97.3)	0.0002(0.0443)	1.6230(98.8)
		δ_2	0.0338(0.0504)	1.6015(98.3)	0.0035(0.0375)	1.6050(99.4)
		δ_3	0.0285(0.0343)	1.3118(99.0)	0.0081(0.0277)	1.3112(99.7)
		β	0.0499(0.0570)	0.5878(83.6)	0.2006(0.0822)	0.6133(85.2)
		δ	0.0590(0.0202)	0.8475(98.3)	0.0265(0.0134)	0.8485(99.6)
		$R(x)$	0.0301(0.0061)	0.4920(96.8)	0.0121(0.0045)	0.5075(99.0)
		$H(x)$	0.1168(0.0719)	1.3371(98.5)	0.0631(0.0409)	1.1658(99.6)
		μ	0.0570(0.0748)	1.6363(92.3)	0.1989(0.2436)	2.5243(98.5)
	$(1.25, 2)$	δ_1	0.0526(0.0535)	1.4407(98.4)	0.0346(0.0382)	1.4317(99.0)
		δ_2	0.0402(0.0508)	1.4424(98.1)	0.0196(0.0365)	1.4339(99.2)
		δ_3	0.0299(0.0282)	1.1886(99.4)	0.0298(0.0232)	1.1723(99.4)
		β	0.0546(0.0483)	0.5175(87.0)	0.1682(0.0632)	0.5337(88.1)
		δ	0.0579(0.0174)	0.7677(98.0)	0.0433(0.0121)	0.7610(99.6)
		$R(x)$	0.0302(0.0052)	0.4557(96.4)	0.0228(0.0039)	0.4489(98.4)
		$H(x)$	0.1127(0.0537)	1.1861(97.8)	0.0291(0.0255)	1.0224(99.8)
		μ	0.0791(0.0471)	1.4591(95.0)	0.0836(0.0821)	1.9171(98.3)

Table 3. The point and interval results for $k = 3$ and CS-II.

(N, M)	(T_i^{min}, T_i^{max})	Par	MLE		MPSE	
			Bias(MSE)	AIL(CP)	Bias(MSE)	AIL(CP)
(N_1, M_1)	$(1, 1.5)$	δ_1	0.2652(0.5393)	1.8963(93.4)	0.0622(0.1322)	1.8797(97.8)
		δ_2	0.0958(0.1030)	1.3045(96.7)	0.0120(0.0398)	1.3041(99.3)
		δ_3	0.1332(0.1362)	1.3742(97.0)	0.0022(0.0426)	1.3664(99.4)
		β	0.1588(0.1196)	0.6370(90.8)	0.1668(0.0891)	0.6989(92.7)
		δ	0.1180(0.0581)	0.8430(93.5)	0.0052(0.0175)	0.8405(99.2)
		$R(x)$	0.0572(0.0124)	0.4896(92.3)	0.0017(0.0052)	0.5461(99.0)
		$H(x)$	0.3132(0.4373)	1.7352(95.1)	0.0575(0.1018)	1.4195(98.9)
		μ	0.1294(0.1038)	1.3136(78.6)	0.2729(0.3115)	2.5060(95.9)
	$(1.25, 2)$	δ_1	0.2117(0.4984)	1.8767(95.6)	0.0328(0.1075)	1.8630(99.2)
		δ_2	0.0930(0.0740)	1.2882(96.8)	0.0130(0.0295)	1.2875(99.6)
		δ_3	0.1139(0.0899)	1.3603(97.5)	0.0078(0.0295)	1.3546(99.7)
		β	0.1734(0.1117)	0.6303(92.3)	0.1561(0.0774)	0.6914(95.0)
		δ	0.1032(0.0425)	0.8341(96.0)	0.0021(0.0128)	0.8322(99.5)
		$R(x)$	0.0517(0.0099)	0.4876(94.9)	0.0050(0.0041)	0.5413(99.5)
		$H(x)$	0.2860(0.3151)	1.7070(97.4)	0.0673(0.0733)	1.3989(99.3)
		μ	0.1379(0.0868)	1.2588(80.8)	0.2471(0.2403)	2.3727(98.1)
(N_1, M_2)	$(1, 1.5)$	δ_1	0.0474(0.0612)	1.2967(97.1)	0.0064(0.0351)	1.2965(99.2)
		δ_2	0.0607(0.0596)	1.2890(97.5)	0.0001(0.0307)	1.2887(99.4)
		δ_3	0.0177(0.0302)	1.0522(98.7)	0.0263(0.0184)	1.0540(99.9)
		β	0.0596(0.0638)	0.5459(95.1)	0.1811(0.0768)	0.5857(95.5)
		δ	0.0361(0.0167)	0.6892(97.6)	0.0109(0.0093)	0.6897(99.7)
		$R(x)$	0.0171(0.0050)	0.4102(96.9)	0.0094(0.0033)	0.4314(99.7)
		$H(x)$	0.0978(0.0952)	1.1908(97.4)	0.0974(0.0502)	1.0371(97.9)
		μ	0.0124(0.0743)	1.3462(90.2)	0.2647(0.2181)	2.0790(97.7)
	$(1.25, 2)$	δ_1	0.0544(0.0548)	1.2657(98.1)	0.0136(0.0307)	1.2639(99.3)
		δ_2	0.0669(0.0586)	1.2720(98.0)	0.0057(0.0286)	1.2714(99.8)
		δ_3	0.0519(0.0374)	1.0417(98.1)	0.0009(0.0194)	1.0429(99.6)
		β	0.1140(0.0761)	0.5304(94.7)	0.1385(0.0633)	0.5692(96.8)
		δ	0.0515(0.0160)	0.6791(98.3)	0.0021(0.0077)	0.6792(99.7)
		$R(x)$	0.0267(0.0048)	0.3960(97.1)	0.0010(0.0027)	0.4174(99.5)
		$H(x)$	0.1507(0.1043)	1.2043(97.5)	0.0599(0.0410)	1.0449(99.0)
		μ	0.0735(0.0601)	1.1688(87.7)	0.1735(0.1331)	1.7850(97.9)

Table 4. The point and interval results for $k = 4$ and CS-I.

(N, M)	(T_i^{min}, T_i^{max})	Par	MLE		MPSE	
			Bias(MSE)	AIL(CP)	Bias(MSE)	AIL(CP)
(N_2, M_3)	$(1, 1.5)$	δ_1	0.1007(0.2820)	2.2659(96.5)	0.0037(0.1118)	2.2769(98.6)
		δ_2	0.0409(0.0541)	1.6053(98.2)	0.0007(0.0399)	1.6093(99.4)
		δ_3	0.0230(0.0344)	1.3101(98.7)	0.0037(0.0285)	1.3099(99.2)
		δ_4	0.0219(0.0244)	1.1334(99.3)	0.0108(0.0208)	1.1313(99.3)
		β	0.0236(0.0371)	0.4777(83.2)	0.1997(0.0679)	0.4934(87.9)
		δ	0.0622(0.0178)	0.7070(97.4)	0.0282(0.0108)	0.7076(99.2)
		$R(x)$	0.0328(0.0051)	0.4068(96.0)	0.0140(0.0035)	0.4214(98.2)
		$H(x)$	0.1049(0.0512)	1.1017(97.8)	0.0631(0.0286)	0.9765(99.5)
		μ	0.0723(0.0473)	1.2787(92.6)	0.1474(0.1140)	1.8582(98.3)
	$(1.25, 2)$	δ_1	0.1190(0.1907)	2.0187(96.0)	0.0266(0.0874)	2.0257(98.3)
		δ_2	0.0323(0.0426)	1.4410(98.7)	0.0091(0.0317)	1.4373(99.2)
		δ_3	0.0257(0.0257)	1.1829(99.1)	0.0227(0.0214)	1.1740(99.4)
		δ_4	0.0174(0.0191)	1.0328(99.4)	0.0240(0.0170)	1.0206(99.8)
		β	0.0189(0.0289)	0.4244(85.9)	0.1800(0.0547)	0.4344(87.8)
		δ	0.0511(0.0118)	0.6433(99.0)	0.0351(0.0080)	0.6390(99.6)
		$R(x)$	0.0276(0.0037)	0.3800(97.9)	0.0189(0.0026)	0.3773(99.1)
		$H(x)$	0.0843(0.0328)	0.9688(98.5)	0.0452(0.0184)	0.8506(100)
		μ	0.0669(0.0318)	1.2175(95.6)	0.0881(0.0525)	1.5700(99.2)
(N_2, M_4)	$(1, 1.5)$	δ_1	0.0172(0.0265)	1.1432(99.2)	0.0109(0.0235)	1.1415(99.2)
		δ_2	0.0158(0.0188)	1.0173(98.8)	0.0136(0.0171)	1.0150(99.1)
		δ_3	0.0092(0.0141)	0.9314(99.8)	0.0104(0.0131)	0.9286(99.9)
		δ_4	0.0125(0.0109)	0.8071(99.6)	0.0178(0.0105)	0.8036(99.6)
		β	0.0221(0.0230)	0.3794(87.5)	0.1355(0.0371)	0.3865(90.8)
		δ	0.0263(0.0051)	0.4725(99.9)	0.0262(0.0046)	0.4712(99.9)
		$R(x)$	0.0144(0.0017)	0.2856(99.7)	0.0145(0.0016)	0.2823(99.7)
		$H(x)$	0.0488(0.0152)	0.7178(99.5)	0.0333(0.0119)	0.6496(99.8)
		μ	0.0391(0.0175)	0.9386(97.6)	0.0589(0.0283)	1.1209(99.7)
	$(1.25, 2)$	δ_1	0.0110(0.0192)	1.0292(99.3)	0.0141(0.0173)	1.0248(99.3)
		δ_2	0.0101(0.0156)	0.9245(99.5)	0.0178(0.0145)	0.9191(99.6)
		δ_3	0.0069(0.0129)	0.8483(99.6)	0.0178(0.0123)	0.8420(99.7)
		δ_4	0.0086(0.0101)	0.7420(99.5)	0.0239(0.0101)	0.7345(99.5)
		β	0.0251(0.0183)	0.3313(89.8)	0.1107(0.0273)	0.3370(93.9)
		δ	0.0174(0.0046)	0.4320(99.5)	0.0272(0.0046)	0.4288(99.4)
		$R(x)$	0.0092(0.0016)	0.2777(99.3)	0.0152(0.0016)	0.2679(99.2)
		$H(x)$	0.0351(0.0097)	0.6570(99.5)	0.0206(0.0074)	0.5893(99.9)
		μ	0.0306(0.0124)	0.9398(99.3)	0.0305(0.0154)	1.0417(99.7)

Table 5. The point and interval results for $k = 4$ and CS-II.

(N, M)	(T_i^{min}, T_i^{max})	Par	MLE		MPSE	
			Bias(MSE)	AIL(CP)	Bias(MSE)	AIL(CP)
(N_2, M_3)	$(1, 1.5)$	δ_1	0.1842(0.4007)	1.8491(94.8)	0.0349(0.1434)	1.8403(98.4)
		δ_2	0.0743(0.0649)	1.2869(98.1)	0.0016(0.0316)	1.2857(99.6)
		δ_3	0.0357(0.0341)	1.0450(98.3)	0.0089(0.0199)	1.0459(99.6)
		δ_4	0.0193(0.0246)	0.9062(99.1)	0.0183(0.0156)	0.9080(99.6)
		β	0.0651(0.0420)	0.4492(94.6)	0.1554(0.0520)	0.4791(95.7)
		δ	0.0440(0.0149)	0.5740(97.9)	0.0108(0.0076)	0.5743(99.7)
		$R(x)$	0.0225(0.0044)	0.3487(97.4)	0.0088(0.0027)	0.3701(99.7)
		$H(x)$	0.1121(0.0811)	1.0504(97.4)	0.0854(0.0396)	0.9240(98.3)
		μ	0.0481(0.0552)	1.0317(86.6)	0.2081(0.1404)	1.5610(98.4)
	$(1.25, 2)$	δ_1	0.2230(0.3639)	1.8516(93.9)	0.0593(0.1259)	1.8423(97.1)
		δ_2	0.0891(0.0719)	1.2806(96.7)	0.0127(0.0340)	1.2795(99.3)
		δ_3	0.0484(0.0316)	1.0336(98.7)	0.0018(0.0177)	1.0344(99.9)
		δ_4	0.0250(0.0221)	0.8964(99.1)	0.0086(0.0131)	0.8978(99.9)
		β	0.0901(0.0499)	0.4413(95.7)	0.1366(0.0492)	0.4710(97.8)
		δ	0.0576(0.0154)	0.5691(97.5)	0.0001(0.0068)	0.5693(99.5)
		$R(x)$	0.0307(0.0045)	0.3402(97.2)	0.0020(0.0023)	0.3621(99.5)
		$H(x)$	0.1471(0.0918)	1.0556(96.7)	0.0618(0.0364)	0.9264(98.3)
		μ	0.0848(0.0516)	0.9482(85.4)	0.1594(0.1054)	1.4355(98.1)
(N_2, M_4)	$(1, 1.5)$	δ_1	0.0084(0.0157)	0.9638(99.3)	0.0145(0.0135)	0.9633(99.7)
		δ_2	0.0078(0.0111)	0.8575(99.8)	0.0114(0.0098)	0.8569(100)
		δ_3	0.0154(0.0093)	0.7853(99.9)	0.0171(0.0084)	0.7845(100)
		δ_4	0.0186(0.0070)	0.6810(100)	0.0184(0.0063)	0.6800(100)
		β	0.0483(0.0157)	0.3391(94.7)	0.1736(0.0417)	0.3499(97.5)
		δ	0.0087(0.0026)	0.4004(100)	0.0112(0.0023)	0.4000(100)
		$R(x)$	0.0061(0.0010)	0.2473(99.9)	0.0075(0.0009)	0.2469(100)
		$H(x)$	0.0378(0.0084)	0.5873(100)	0.1023(0.0162)	0.5429(98.5)
		μ	0.0623(0.0182)	0.9306(99.9)	0.1655(0.0479)	1.1035(100)
	$(1.25, 2)$	δ_1	0.0071(0.0176)	0.9115(99.2)	0.0027(0.0146)	0.9103(99.4)
		δ_2	0.0107(0.0115)	0.8174(99.6)	0.0108(0.0098)	0.8158(99.8)
		δ_3	0.0114(0.0098)	0.7476(99.7)	0.0095(0.0084)	0.7457(99.9)
		δ_4	0.0149(0.0067)	0.6487(99.9)	0.0101(0.0058)	0.6463(99.9)
		β	0.0757(0.0171)	0.3063(95.1)	0.1865(0.0447)	0.3161(97.6)
		δ	0.0061(0.0027)	0.3813(100)	0.0051(0.0023)	0.3803(100)
		$R(x)$	0.0045(0.0010)	0.2395(99.8)	0.0038(0.0008)	0.2370(100)
		$H(x)$	0.0475(0.0091)	0.5394(99.8)	0.1008(0.0155)	0.4988(97.2)
		μ	0.0746(0.0200)	0.9448(99.7)	0.1597(0.0435)	1.0828(99.9)

Furthermore, to simulate the effect of the DDTF, random noise is introduced into the generated samples using a normal distribution with mean 0 and variance $0.001 \times i$, where $i = 1, \ldots, k$. This procedure enables the generation of BIAPTIIHC data that reflect different test facilities. To quantify the degree of heterogeneity across groups, we introduce a measure called the CSI, which is based on the overlap of the confidence intervals associated with the scale parameters δ_i, $i = 1, \ldots, k$. The CSI is defined as

$$\text{CSI} = \frac{\min(U_1, \ldots, U_k) - \max(L_1, \ldots, L_k)}{\max(U_1, \ldots, U_k) - \min(L_1, \ldots, L_k)} \times 100,$$

where L_i and U_i denote the lower and upper confidence bounds of δ_i for the i-th group. The numerator represents the length of the common overlapping region shared by all confidence intervals, while the denominator represents the total span covered by the union of these intervals. Therefore, the CSI measures the proportion of the total interval range that is jointly shared by all groups. If the confidence intervals overlap substantially, the numerator approaches the denominator and the CSI approaches 100%, indicating strong similarity among the groups. If the intervals exhibit only partial overlap, the CSI takes intermediate values between 0% and 100%. When there is no common overlap among the intervals; in such cases, the CSI is set to zero, reflecting complete separation and strong heterogeneity. Thus, the CSI provides a normalized and easily interpretable measure of group-level similarity, allowing a direct quantitative assessment of heterogeneity rather than relying solely on visual inspection of interval overlap. For each simulated dataset, the CSI is computed using the ACIs of the estimated scale parameters, and the resulting values are then averaged over the 1000 replications to assess the overall degree of similarity across groups. These results are displayed in Table 6.

Based on the results reported in Tables 2–6, the following main observations can be drawn:

(1) In general, both estimation methods perform well in estimating the model parameters, RCs, and DDTF, for both point and interval estimation.
(2) For the parameters $\delta_i, i = 1, \ldots, k$, and the derived reliability measures $R(x)$ and $H(x)$, the MPSEs exhibit smaller bias and lower MSE values than the MLEs. However, the MLEs perform better for the shape parameter β and for the MTTF μ, often achieving slightly smaller bias and MSE values.
(3) It is worth noting that the superior performance of the MPS method in several small-sample configurations can be attributed to its robustness properties. Under complex censoring structures and limited effective sample sizes, the likelihood function may exhibit flatness or skewness. In such cases, the MLEs can become sensitive to sample fluctuations and tail behavior. In contrast, the MPS method is based on the distribution of cumulative probabilities and tends to be less influenced by extreme observations and censoring irregularities.
(4) Increasing the sample size (n_i) or the number of observed failures (m_i) consistently improves estimation accuracy by reducing both bias and MSE and by shortening the confidence intervals. Similarly, employing higher threshold values $(T_i^{\min}, T_i^{\max}) = (1.25, 2)$ enhances precision for both estimators by decreasing the MSE and AIL values.
(5) Regarding interval estimation, the ACIs constructed from both estimators achieve satisfactory CPs close to the nominal level. The MPSE-based ACIs generally produce shorter AILs in most cases and slightly higher CPs, especially for the δ_i parameters and the $R(x)$ and $H(x)$ measures. Conversely, the MLE-based ACIs yield the smallest AIL values for the shape parameter β and the MTTF μ in all cases.

(6) In most cases, the MSE values are smaller under CS-I than those obtained under CS-II for both estimation methods. On the other hand, the AILs obtained using CS-II are generally shorter than those from CS-I, indicating a trade-off between estimation precision and interval width depending on the censoring scheme.
(7) For $k = 3$, the CSI values range roughly between 50% and 63%, reflecting moderate similarity among the test facilities.
(8) For $k = 4$, the CSI values decrease to approximately 37%–56%, indicating increased heterogeneity as the number of facilities grows.
(9) The MPSE-based CSI values are consistently higher than those of the MLEs, suggesting more coherent inference across different facilities. This observation also explains the superior performance of the MPSEs for estimating the RF and HRF compared with the MLEs.
(10) It is evident that as n_i and m_i increase, the CSI values also increase in all scenarios, indicating more consistent inference and stronger similarity among the facilities.
(11) These findings confirm that the DDTF effects cannot be ignored, as facility-specific deviations have a significant influence on the accuracy of the estimated reliability characteristics.

Table 6. Coverage similarity index for $k = 3$ and 4.

k	(N, M)	(T_i^{min}, T_i^{max})	CS	MLE	MPSE
3	(N_1, M_1)	$(1, 1.5)$	I	53.17	56.94
			II	50.28	57.89
		$(1.25, 2)$	I	53.09	56.54
			II	51.36	58.87
	(N_1, M_2)	$(1, 1.5)$	I	59.55	62.07
			II	57.94	63.71
		$(1.25, 2)$	I	59.62	62.01
			II	57.39	63.71
4	(N_2, M_3)	$(1, 1.5)$	I	40.07	42.41
			II	37.70	42.25
		$(1.25, 2)$	I	40.65	42.80
			II	37.25	41.60
	(N_2, M_4)	$(1, 1.5)$	I	53.45	54.36
			II	55.52	56.87
		$(1.25, 2)$	I	54.71	55.32
			II	54.21	55.96

6. Real-world data application

In this section, a real data example is analyzed to demonstrate the applicability of the proposed BIAPTIIHC scheme and to evaluate the performance of the two employed estimation methods. The dataset concerns the survival times of cancer patients undergoing treatment, where a subset of

patients received supplemental ascorbate in addition to conventional therapy, while the remaining patients received the same treatment without ascorbate supplementation. Average survival times are reported for both the ascorbate-treated and the matched control groups across several cancer types, including ovary, breast, and kidney cancers, among others. In this application, the blocks correspond to biologically distinct cancer subtypes rather than to separate hospitals or research stages. All patients were drawn from the same clinical study; however, the ovary, breast, and kidney cancer groups represent independent subpopulations with potentially different survival characteristics. Accordingly, each cancer type is treated as a separate block within the proposed framework. This interpretation aligns with the general block structure, where independent groups may exhibit heterogeneous lifetime behavior while sharing a common modeling structure.

The survival times are measured from the date of the patients' initial hospital attendance for cancer treatment at the terminal stage of their disease. This dataset has been previously analyzed in different contexts, see, for example, Cameron and Pauling [42]. Recently, Singh et al. [26] analyzed this dataset under the BAPTIIHC scheme. In their study, the original survival times for the three cancer groups, ovary, breast, and kidney, were transformed by dividing each observation within a group by its respective group mean. The sample sizes for the three cancer groups are $n_i = (27, 50, 30)$, corresponding to the ovary, breast, and kidney categories, respectively. Singh et al. [26] demonstrated that the Weibull distribution provides an adequate fit for this dataset based on several goodness-of-fit criteria. For the three cancer groups, ovary, breast, and kidney, the Kolmogorov–Smirnov (K–S) statistics and their corresponding p-values were reported as 0.0960 (0.9644), 0.0844 (0.8678), and 0.1174 (0.8024), respectively. These results show the suitability of the Weibull distribution to model the three groups of cancer data.

The cancer survival dataset provides a suitable context for illustrating the proposed BIAPTIIHC scheme for several reasons. First, the data are naturally partitioned into distinct cancer subtypes, which can be treated as independent experimental groups under a block framework. Second, survival studies often involve incomplete follow-up and administrative termination times, making hybrid and time-controlled censoring structures practically relevant. Third, potential biological heterogeneity across cancer types justifies the use of group-specific scale parameters within a common modeling framework. Therefore, this dataset offers a realistic setting to demonstrate both the flexibility of the proposed censoring design and the practical utility of the CSI in quantifying inter-group variation. Although the BIAPTIIHC framework was originally motivated by multi-facility reliability experiments, its structure applies more generally to independent experimental blocks or subpopulations that may exhibit heterogeneous lifetime behavior. In the present application, the block structure arises from biological heterogeneity across different cancer types (ovary, breast, and kidney), rather than from operational differences across physical testing facilities. Accordingly, the DDTF in this context reflects variation in survival characteristics across cancer subtypes, and the CSI quantifies the degree of overlap among their estimated scale parameters.

Singh et al. [26] employed the original dataset to generate a BAPTIIHC sample under different configurations for each cancer group. Since the proposed BIAPTIIHC scheme generalizes the BAPTIIHC scheme by introducing an additional time threshold, $T_i^{\max}$, we adopted the same experimental design used by Singh et al. [26], while incorporating new values for $T_i^{\max}$ to generate a BIAPTIIHC sample from the original data. The applied testing plan, along with the corresponding values of J_i, Q_i, τ_i, and $R_i^{\star}$, is presented in Table 7, while the generated samples are displayed in

Table 8. It can be observed from Table 7 that all three tests terminate at $T_i^{\max}$ with $J_i < m_i$, indicating that the termination occurs before the planned number of failures is reached.

Table 7. The used testing plan and the values of J_i, Q_i, τ_i, and $R_i^{\star}$.

Cancer	m_i	(T_i^{min}, T_i^{max})	$\mathcal{R}_i$	J_i	Q_i	τ_i	$R_i^{\star}$
Ovary	23	(1.5,2)	$(4, 0 * 22)$	19	16	2	4
Breast	37	(2,3)	$(0 * 18, 13, 0 * 18)$	34	29	3	3
Kidney	25	(1.2,1.5)	$(0 * 24, 5)$	21	18	1.5	9

Table 8. BIAPTIIHC cancer data.

Cancer	Survival data
Ovary	0.3662, 0.3865, 0.4272, 0.4272, 0.4476, 0.4476, 0.6510, 0.6714, 0.7324, 0.7731, 0.7935, 0.8138, 0.9766, 0.9969, 1.0783, 1.3835, 1.7294, 1.7498, 1.9736
Breast	0.0203, 0.0406, 0.0406, 0.0609, 0.0812, 0.1218, 0.1218, 0.1421, 0.2030, 0.2437, 0.2437, 0.2843, 0.2843, 0.3046, 0.3046, 0.3046, 0.3249, 0.3249, 0.9748, 1.0154, 1.0560, 1.1169, 1.2388, 1.3200, 1.4012, 1.4419, 1.5434, 1.6450, 1.9090, 2.0511, 2.0714, 2.1730, 2.2136, 2.6604
Kidney	0.0396, 0.0992, 0.1190, 0.1587, 0.1587, 0.1587, 0.2778, 0.3174, 0.3373, 0.5158, 0.5357, 0.5753, 0.5753, 0.6150, 0.8134, 0.9722, 1.0912, 1.1904, 1.2896, 1.3492, 1.3690

Based on the generated BIAPTIIHC cancer data presented in Table 8, the model parameters and corresponding RCs are estimated using both estimation methods. The MLEs and MPSEs, along with their associated standard errors (SEs), are reported in Table 9. The estimates of the RF and HRF are evaluated at mission time 0.5. Furthermore, the ACIs for the different quantities are constructed based on both MLEs and MPSEs, and their lower bounds, upper bounds, and interval lengths are also summarized in Table 9. A comparison between the two estimation methods in this real-data application reveals several notable observations. For the scale parameters δ_i and the overall scale parameter δ, both methods yield very similar point estimates and SEs, indicating stable and consistent inference under the proposed censoring structure. The interval lengths obtained from the maximum product of spacings method are slightly shorter for δ_1 and δ_3, while remaining comparable for δ_2, suggesting marginally improved precision in estimating scale-related parameters. For the shape parameter β, the MPS method produces a slightly narrower confidence interval than maximum likelihood, although the point estimates remain close. In contrast, for the MTTF, the maximum likelihood method provides a shorter interval length, indicating better precision for this derived measure in this dataset. For the RF and HRF, both methods produce nearly identical point estimates and very similar interval widths, demonstrating

robustness of the reliability inference under both estimation approaches. Overall, the real-data findings are consistent with the simulation results, where the MPS method showed competitive or slightly superior performance for scale-related quantities, while maximum likelihood performed favorably for the MTTF.

Table 9. The point and interval results for BIAPTIIHC cancer data.

Par	MLE				MPSE			
	Estimate(SE)	Lower	Upper	Length	Estimate(SE)	Lower	Upper	Length
δ_1	0.716(0.164)	0.393	1.038	0.646	0.704(0.161)	0.386	1.021	0.635
δ_2	0.653(0.114)	0.428	0.879	0.451	0.660(0.114)	0.434	0.887	0.453
δ_3	0.801(0.176)	0.458	1.144	0.686	0.786(0.170)	0.449	1.122	0.673
β	1.057(0.105)	0.853	1.261	0.408	0.968(0.100)	0.776	1.161	0.385
δ	0.702(0.084)	0.538	0.867	0.329	0.701(0.083)	0.537	0.864	0.326
$R(x)$	0.713(0.037)	0.641	0.786	0.144	0.713(0.037)	0.626	0.772	0.145
$H(x)$	0.713(0.083)	0.551	0.877	0.326	0.714(0.081)	0.535	0.852	0.318
μ	1.367(0.162)	1.049	1.684	0.634	1.465(0.196)	1.080	1.850	0.770

To evaluate the degree of heterogeneity across the cancer subtypes, the CSI was computed using both estimation methods. The CSI values were found to be 56.059% for the MLEs and 59.511% for the MPSEs. The higher CSI obtained from the MPSEs indicates a greater overlap among the confidence intervals of the estimated scale parameters across the three cancer groups, suggesting more consistent inference under this method. Although the interval estimates exhibit partial overlap, the CSI values clearly indicate that non-negligible heterogeneity exists among the survival behaviors of the ovary, breast, and kidney cancer subtypes. This heterogeneity has a noticeable impact on the accuracy and stability of reliability estimation and therefore should not be ignored in practical analysis. Figures 1 and 2 display the plots of the ACIs based on the MLEs and MPSEs, respectively, for δ_i $(i = 1, 2, 3)$. The plots visually confirm partial overlap among the interval estimates, further supporting the presence of meaningful biological variation across the cancer groups.

Overall, the CSI values around 56%–60% indicate a moderate degree of similarity among the scale parameters of the three cancer groups. This suggests that although the survival behaviors are not completely distinct, there exists meaningful heterogeneity across the cancer types that should be considered in reliability modeling. Ignoring such variation and assuming a common scale parameter could lead to biased reliability assessment and misleading conclusions regarding survival characteristics. Therefore, the CSI provides practical guidance by quantifying the extent to which group-specific modeling is warranted.

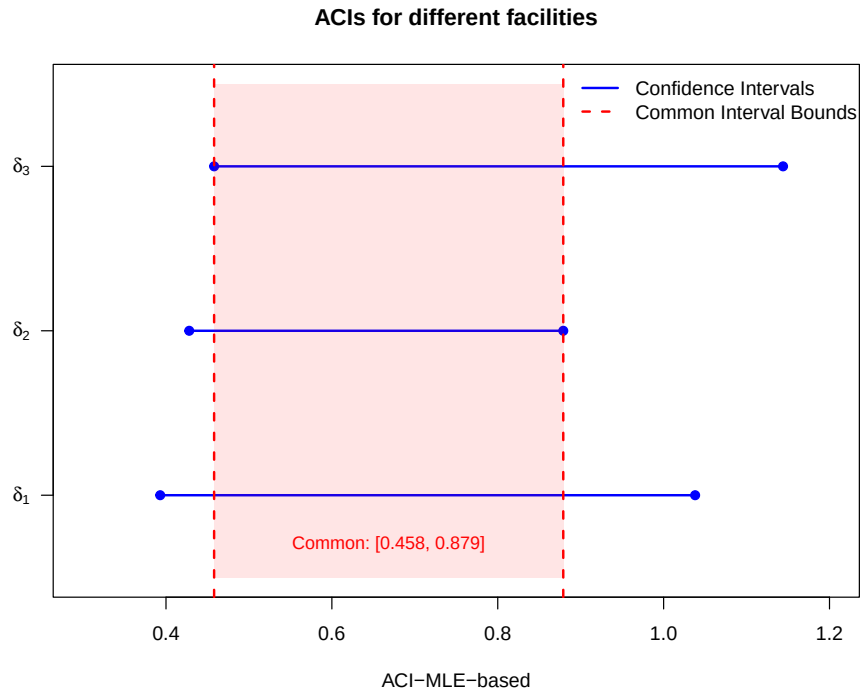

Figure 1. Various ACIs-MLE-based for δ_i.

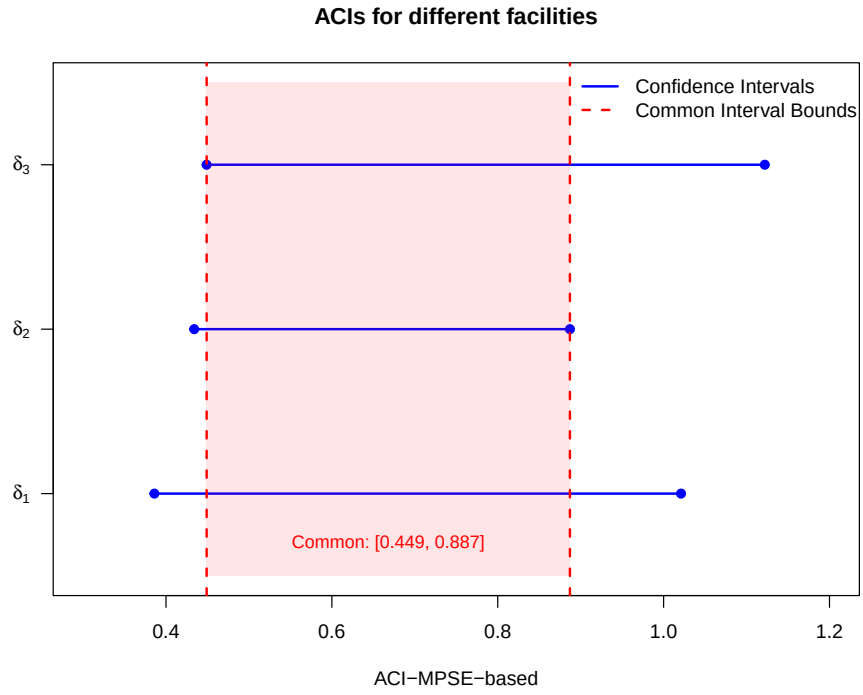

Figure 2. Various ACIs-MPSE-based for δ_i.

7. Conclusions

In this study, a new censoring methodology called the block improved adaptive progressive Type-II hybrid censoring scheme was proposed and investigated as an effective approach for improving the efficiency of life-testing experiments conducted across multiple testing facilities. The proposed scheme generalizes several well-known censoring plans, including the conventional block progressive Type-II and adaptive progressive Type-II hybrid censoring schemes, by introducing an additional upper time threshold to provide greater flexibility in experimental design. The Weibull distribution was adopted as the lifetime model, and its parameters and main reliability characteristics, such as the reliability function, the hazard rate function, and the mean time to failure, were estimated using two classical methods: the maximum likelihood estimation method and the maximum product of spacings estimation method. Both point estimates and confidence interval estimates were derived for comparison. To quantify the differences among multiple testing facilities, a new measure named the coverage similarity index was developed. This measure evaluates the extent of overlap among confidence intervals of facility-specific estimates and thus provides insight into the degree of similarity or discrepancy across testing environments. A comprehensive simulation study was performed under various configurations of sample sizes, numbers of observed failures, censoring schemes, and time thresholds to assess the performance of the proposed estimators. The findings revealed that both estimation methods perform well overall. The maximum product of spacings method generally provides smaller bias and mean square error for most parameters and reliability characteristics, while the maximum likelihood method performs slightly better for estimating the shape parameter and the mean time to failure. Larger sample sizes, higher numbers of observed failures, and longer threshold times improve estimation accuracy and reduce interval lengths. An application to real cancer survival data involving three groups, ovary, breast, and kidney, demonstrated the practical usefulness of the proposed scheme. The results emphasized the significance of accounting for variability between testing facilities, as this variation meaningfully affects the precision of reliability estimates.

Although the proposed framework provides flexible modeling under complex censoring structures, several limitations should be acknowledged. First, the real-data application is based on a specific cancer survival dataset, and the numerical findings obtained from this example cannot be directly generalized to other medical or reliability contexts without further validation. Estimator performance may vary depending on sample size, censoring intensity, group structure, and the underlying lifetime distribution. Second, all inferential procedures were developed under the assumption that the lifetime distribution follows a Weibull model. While the Weibull distribution is flexible and widely used, it may not adequately capture more complex hazard behaviors, such as bathtub-shaped or unimodal patterns. Consequently, model misspecification could influence parameter estimation and reliability inference. Assessing robustness under alternative lifetime models remains an important topic for future investigation. Third, the proposed framework assumes a common shape parameter across groups and allows heterogeneity only in the scale parameters. Although this assumption is reasonable in many practical situations, a more general formulation allowing both parameters to vary across groups may provide additional modeling flexibility. Finally, although several representative simulation configurations were examined, the study does not exhaust all possible parameter settings or heterogeneity structures. In particular, facility-level variation was introduced through a controlled perturbation mechanism within the Weibull framework. Broader simulation designs incorporating

alternative heterogeneity mechanisms, additional threshold configurations, and diverse parameter combinations could provide deeper insight into the robustness and stability of the proposed estimators.

In future research, the proposed block-based improved adaptive censoring scheme may be extended to more flexible lifetime distributions, including generalized Weibull families and competing risks models. Bayesian estimation approaches could also be developed under the proposed design to incorporate prior information and address small-sample uncertainty. In addition, formal hypothesis testing procedures for assessing group-level heterogeneity could complement the coverage similarity index and provide further inferential tools. Another promising direction for future research is to extend the proposed block-based adaptive censoring framework to recurrent event settings, particularly in the context of panel count data, where only the number of events occurring between inspection times is observed. Recent methodological developments in this area, such as those of Zhu et al. [43] and Wang et al. [44], provide a useful foundation for such extensions. Another important direction for future research is the development of Bayesian inference procedures under the proposed scheme. While the present study focuses on classical likelihood-based estimation, a Bayesian extension would allow the incorporation of prior information, hierarchical modeling of group-level heterogeneity, and improved uncertainty quantification, particularly in small-sample settings. In multi-group reliability and survival contexts, Bayesian hierarchical structures could naturally accommodate facility-specific parameters while maintaining a unified modeling framework. Moreover, recent advances in Bayesian degradation modeling, recursive prediction, and heterogeneous system analysis suggest promising methodological avenues for integrating adaptive block censoring mechanisms with modern Bayesian techniques (see, for example, Zhu et al. [45], Xu and Wang [46], and Yin et al. [47]). Extending the proposed scheme within such frameworks represents a meaningful and practically relevant topic for future investigation.

Author contributions

Mazen Nassar: Conceptualization, methodology, investigation, writing – original draft, software; Refah Alotaibi: Conceptualization, methodology, investigation, funding acquisition, writing – original draft. All authors have read and approved the final version of the manuscript for publication.

Use of Generative-AI tools declaration

The authors declare that they have not used Artificial Intelligence (AI) tools in the creation of this article.

Funding

This research was funded by Princess Nourah bint Abdulrahman University Researchers Supporting Project number (PNURSP2026R50), Princess Nourah bint Abdulrahman University, Riyadh, Saudi Arabia.

Data availability

The authors confirm that the data supporting the findings of this study are available within the article.

Conflict of interest

The authors declare no conflicts of interest.

References

1. H. K. T. Ng, P. S. Chan, N. Balakrishnan, Estimation of parameters from progressively censored data using EM algorithm, *Comput. Stat. Data Anal.*, **39** (2002), 371–386. https://doi.org/10.1016/s0167-9473(01)00091-3
2. D. Kundu, Bayesian inference and life testing plan for the Weibull distribution in presence of progressive censoring, *Technometrics*, **50** (2008), 144–154. https://doi.org/10.1198/004017008000000217
3. A. H. I. Lee, C. W. Wu, T. C. Wang, M. H. Kuo, Construction of acceptance sampling schemes for exponential lifetime products with progressive Type II right censoring, *Reliab. Eng. Syst. Safe.*, **243** (2024), 109843. https://doi.org/10.1016/j.ress.2023.109843
4. D. Kundu, A. Joarder, Analysis of Type-II progressively hybrid censored data, *Comput. Stat. Data Anal.*, **50** (2006), 2509–2528. https://doi.org/10.1016/j.csda.2005.05.002
5. H. K. T. Ng, D. Kundu, P. S. Chan, Statistical analysis of exponential lifetimes under an adaptive Type-II progressive censoring scheme, *Nav. Res. Log.*, **56** (2009), 687–698. https://doi.org/10.1002/nav.20371
6. J. Ren, W. Gui, Statistical analysis of adaptive type-II progressively censored competing risks for Weibull models, *Appl. Math. Model.*, **98** (2021), 323–342. https://doi.org/10.1016/j.apm.2021.05.008
7. H. Haj Ahmad, M. M. Salah, M. S. Eliwa, Z. Ali Alhussain, E. M. Almetwally, E. A. Ahmed, Bayesian and non-Bayesian inference under adaptive type-II progressive censored sample with exponentiated power Lindley distribution, *J. Appl. Stat.*, **49** (2022), 2981–3001. https://doi.org/10.1080/02664763.2021.1931819
8. R. Alotaibi, M. Nassar, A. Elshahhat, Computational analysis of XLindley parameters using adaptive Type-II progressive hybrid censoring with applications in chemical engineering, *Mathematics*, **10** (2022), 3355. https://doi.org/10.3390/math10183355
9. S. Dutta, S. Dey, S. Kayal, Bayesian survival analysis of logistic exponential distribution for adaptive progressive Type-II censored data, *Comput. Stat.*, **39** (2024), 2109–2155. https://doi.org/10.1007/s00180-023-01376-y
10. Q. Lv, Y. Tian, W. Gui, Statistical inference for Gompertz distribution under adaptive type-II progressive hybrid censoring, *J. Appl. Stat.*, **51** (2024), 451–480. https://doi.org/10.1080/02664763.2022.2136147

11. M. Nassar, Adaptive progressive censoring in reliability and survival analysis: methods, design, and practice, *J. Stat. Models Methods*, **1** (2025), 74–97. https://doi.org/10.65905/vq1mfz74
12. W. Yan, P. Li, Y. Yu, Statistical inference for the reliability of Burr-XII distribution under improved adaptive Type-II progressive censoring, *Appl. Math. Model.*, **95** (2021), 38–52. https://doi.org/10.1016/j.apm.2021.01.050
13. S. Dutta, S. Kayal, Inference of a competing risks model with partially observed failure causes under improved adaptive type-II progressive censoring, *Proceedings of the Institution of Mechanical Engineers, Part O: Journal of Risk and Reliability*, **237** (2023), 765–780. https://doi.org/10.1177/1748006x221104555
14. M. Nassar, A. Elshahhat, Estimation procedures and optimal censoring schemes for an improved adaptive progressively type-II censored Weibull distribution, *J. Appl. Stat.*, **51** (2024), 1664–1688. https://doi.org/10.1080/02664763.2023.2230536
15. L. Zhang, R. Yan, Parameter estimation of Chen distribution under improved adaptive type-II progressive censoring, *J. Stat. Comput. Simul.*, **94** (2024), 2830–2861. https://doi.org/10.1080/00949655.2024.2358828
16. M. Irfan, S. Dutta, A. K. Sharma, Statistical inference and optimal plans for improved adaptive type-II progressive censored data following Kumaraswamy-G family of distributions, *Phys. Scr.*, **100** (2025), 025213. https://doi.org/10.1088/1402-4896/ada216
17. A. Dey, S. Kayal, Statistical inference of a Chen lifetime competing risks model based on improved adaptive Type-II progressive censored data, *Qual. Reliab. Eng. Int.*, **42** (2025), 185–211. https://doi.org/10.1002/qre.70060
18. M. Nassar, R. Alotaibi, A. Elshahhat, Reliability analysis at usual operating settings for Weibull constant-stress model with improved adaptive Type-II progressively censored samples, *AIMS Math.*, **9** (2024), 16931–16965. https://doi.org/10.3934/math.2024823
19. M. V. Ahmadi, M. Doostparast, J. Ahmadi, Block censoring scheme with two-parameter exponential distribution, *J. Stat. Comput. Simul.*, **88** (2018), 1229–1251. https://doi.org/10.1080/00949655.2018.1426763
20. T. Zhu, Reliability estimation for two-parameter Weibull distribution under block censoring, *Reliab. Eng. Syst. Safe.*, **203** (2020), 107071. https://doi.org/10.1016/j.ress.2020.107071
21. R. Kumari, Y. M. Tripathi, R. K. Sinha, L. Wang, Reliability estimation for bathtub-shaped distribution under block progressive censoring, *Math. Comput. Simul.*, **213** (2023), 237–260. https://doi.org/10.1016/j.matcom.2023.06.007
22. R. Kumari, Y. M. Tripathi, L. Wang, R. K. Sinha, Reliability estimation for Kumaraswamy distribution under block progressive type-II censoring, *Statistics*, **58** (2024), 142–175. https://doi.org/10.1080/02331888.2024.2301736
23. L. Wang, S. J. Wu, H. Lin, Y. M. Tripathi, Inference for block progressive censored competing risks data from an inverted exponentiated exponential model, *Qual. Reliab. Eng. Int.*, **39** (2023), 2736–2764. https://doi.org/10.1002/qre.3382
24. K. Singh, Y. M. Tripathi, C. Lodhi, L. Wang, Inference for unit inverse Weibull

distribution under block progressive type-II censoring, *J. Stat. Theory Pract.*, **18** (2024), 42. https://doi.org/10.1007/s42519-024-00395-2

25. C. Lodhi, A. K. Gangopadhyay, P. Bhattacharya, Likelihood and pivotal-based reliability inference for inverse exponentiated Rayleigh distribution under block progressive censoring, *Qual. Technol. Quant. Manage.*, **22** (2025), 779–804. https://doi.org/10.1080/16843703.2024.2400435
26. K. Singh, Y. M. Tripathi, L. Wang, S. J. Wu, Analysis of block adaptive Type-II progressive hybrid censoring with Weibull distribution, *Mathematics*, **12** (2024), 1–21. https://doi.org/10.3390/math12244026
27. W. Weibull, A statistical distribution function of wide applicability, *J. Appl. Mech.*, **18** (1951), 293–297. https://doi.org/10.1115/1.4010337
28. H. K. T. Ng, Z. Wang, Statistical estimation for the parameters of Weibull distribution based on progressively type-I interval censored sample, *J. Stat. Comput. Simul.*, **79** (2009), 145–159. https://doi.org/10.1080/00949650701648822
29. C. B. Guure, N. A. Ibrahim, Bayesian analysis of the survival function and failure rate of Weibull distribution with censored data, *Math. Probl. Eng.*, **2012** (2012), 329489. https://doi.org/10.1155/2012/329489
30. M. Ajmal, M. Y. Danish, I. A. Arshad, Objective Bayesian analysis for Weibull distribution with application to random censorship model, *J. Stat. Comput. Simul.*, **92** (2022), 43–59. https://doi.org/10.1080/00949655.2021.1931210
31. J. Kazempoor, A. Habibirad, A. A. Nadi, G. R. M. Borzadaran, Statistical inferences for the Weibull distribution under adaptive progressive type-II censoring plan and their application in wind speed data analysis, *Stat., Optim. Inf. Comput.*, **11** (2023), 829–852. https://doi.org/10.19139/soic-2310-5070-1501
32. A. Fathi, Inference for Weibull distribution based on adaptive progressive first-failure censored sampling, *J. Stat. Comput. Simul.*, **95** (2025), 3883–3904. https://doi.org/10.1080/00949655.2025.2547972
33. D. N. Prabhakar Murthy, M. Xie, R. Jiang, *Weibull models*, New York, NY, USA: John Wiley & Sons, 2003. https://doi.org/10.1002/047147326X
34. C. D. Lai, D. N. P. Murthy, M. Xie, Weibull distributions, *WIREs Comput. Stat.*, **3** (2011), 282–287. https://doi.org/10.1002/wics.157
35. M. A. Abdelaziz, G. M. Cordeiro, Z. M. Nofal, A. Z. Afify, A comprehensive survey of Weibull-based families, *J. Stat. Models Methods*, **1** (2025), 98–118. https://doi.org/10.65905/zr8pgy41
36. R. C. H. Cheng, N. A. K. Amin, Estimating parameters in continuous univariate distributions with a shifted origin, *J. R. Stat. Soc.: Ser. B (Methodol.)*, **45** (1983), 394–403. https://doi.org/10.1111/j.2517-6161.1983.tb01268.x
37. K. Ghosh, S. R. Jammalamadaka, A general estimation method using spacings, *J. Stat. Plan. Infer.*, **93** (2001), 71–82. https://doi.org/10.1016/s0378-3758(00)00160-9
38. S. Anatolyev, G. Kosenok, An alternative to maximum likelihood based on spacings, *Economet. Theory*, **21** (2005), 472–476. https://doi.org/10.1017/s0266466605050255

39. R. K. Singh, S. K. Singh, U. Singh, Maximum product spacings method for the estimation of parameters of generalized inverted exponential distribution under progressive Type II censoring, *J. Stat. Manage. Syst.*, **19** (2016), 219–245. https://doi.org/10.1080/09720510.2015.1023553
40. G. Volovskiy, U. Kamps, Maximum product of spacings prediction of future record values, *Metrika*, **83** (2020), 853–868. https://doi.org/10.1007/s00184-020-00767-1
41. M. S. U. R. Khan, Z. Hussain, S. Sher, M. Amjad, F. Baig, I. Ahmad, et al., A comparative analysis of L-moments, maximum likelihood, and maximum product of spacing methods for the four-parameter kappa distribution in extreme value analysis, *Sci. Rep.*, **15** (2025), 164. https://doi.org/10.1038/s41598-024-84056-1
42. E. Cameron, L. Pauling, Supplemental ascorbate in the supportive treatment of cancer: reevaluation of prolongation of survival times in terminal human cancer, *Proc. Natl. Acad. Sci. USA*, **75** (1978), 4538–4542. https://doi.org/10.1073/pnas.75.9.4538
43. L. Zhu, S. Choi, Y. Li, X. Huang, J. Sun, L. L. Robison, Statistical analysis of clustered mixed recurrent-event data with application to a cancer survivor study, *Lifetime Data Anal.*, **26** (2020), 820–832. https://doi.org/10.1007/s10985-020-09500-6
44. W. Wang, Y. Wang, X. Zhao, Estimation and inference for fixed center effects on panel count data, *Stat. Papers*, **67** (2026), 27. https://doi.org/10.1007/s00362-026-01807-0
45. D. Zhu, A. Xu, Z. Chen, S. Ding, G. Fang, An online Bayesian framework for identifying latent system degradation states, *IEEE Trans. Reliab.*, **75** (2026), 542–554. https://doi.org/10.1109/tr.2025.3647489
46. A. Xu, W. Wang, Recursive Bayesian prediction of remaining useful life for gamma degradation process under conjugate priors, *Scand. J. Stat.*, **53** (2026), 175–206. https://doi.org/10.1111/sjos.70031
47. H. Yin, Y. Wang, A. Xu, Kernel-based marginal testing for covariate effects in high-dimensional settings, *Scand. J. Stat.*, **53** (2026), 498–531. https://doi.org/10.1111/sjos.70049

AIMS Press